526

NOT FOR PUBLICATION

INDC(JAP) 13L
EANDC(J) 26L

PROGRESS REPORT

(July 1971 to June 1972 inclusive)

August 1972

edited by

T. Momota

aided by

T. Fuketa and S. Tanaka

Japanese Nuclear Data Committee

Japan Atomic Energy Research Institute

Tokai Research Establishment

Tokai-mura, Ibaraki-ken, Japan

NOT FOR PUBLICATION

INDC(JAP) 13L
EANDC(J) 26L

PROGRESS REPORT

(July 1971 to June 1972 inclusive)

August 1972

edited by

T. Momota

aided by

T. Fuketa and S. Tanaka

Japanese Nuclear Data Committee

Japan Atomic Energy Research Institute

Tokai Research Establishment

Tokai-mura, Ibaraki-ken, Japan

Editor's Note

This is a collection of reports which have been submitted to the Japanese Nuclear Data Committee at the Committee's request. The request was addressed to the following individuals who might represent or be in touch with groups doing researches related to the nuclear data of interest to the development of the nuclear energy program.

Although the editor tried not to miss any appropriate addressees, there might have been some oversight. Meanwhile, contribution of a report rested with discretion of its author. The coverage of this document, therefore, might not be uniform over the related field of research.

This edition covers a period of July 1, 1971 to June 30, 1972. The informations herein contained are of a nature of "Private Communication." They should not be quoted without author's permission.

Addressees of the request (in Alphabetical order):

1) Electrotechnical Laboratory

   Tanashi Branch / 5-4-1, Mukaidai, Tanashi, Tokyo

   (E. Teranishi)

2) Hiroshima University

   Faculty of Science / 1-1-89 Higashi-senda, Hiroshima

   (N. Ryu)

3) Hitachi Ltd.

   Atomic Energy Research Laboratory / Oozenji, Tama-ku, Kawasaki-shi, Kanagawa

   (H. Yamamoto, M. Yamamoto)

4) Japan Atomic Energy Research Institute

   Tokai Research Establishment / Tokai-mura, Naka-gun, Ibaraki

   (H. Amano, T. Asami, J. Hirota, T. Ishimori, S. Katsuragi, H. Natsume, K. Nishimura, E. Sakai, H. Takekoshi, K. Tsukada, K. Ueno, et al.)

5) Konan University

   Faculty of Science / Okamoto, Motoyama-cho, Higashinada-ku, Kobe-shi, Hyogo

   (K. Yuasa)

6) Kyoto University

   a) Faculty of Science / Kitashirakawa Oiwake-cho, Sakyo-ku, Kyoto

      (J. Muto)

   b) Keage Laboratory of Nuclear Science, Institute for Chemical Research / 2 Torii-cho, Awataguchi, Sakyo-ku, Kyoto

      (T. Yanabu)

   c) Research Reactor Institute / Kumatori, Sennan-gun, Osaka

      (T. Shibata, K. Okano)

7) Kyushu University

a) Faculty of Science / Hakozaki-cho, Fukuoka

(A. Isoya)

b) Faculty of Engineering / Hakozaki-cho, Fukuoka

(M. Sonoda)

8) Mitsubishi Atomic Power Industries Inc.

Engineering and Development Division / Kitafukuro, Omiya-shi, Saitama

(T. Iwaki)

9) Nagoya University

Fuculty of Engineering / Furo-cho Chigusa-ku, Nagoya

(T. Katoh)

10) Niigata University

Faculty of Science / 8050 Nino-cho, Igarashi, Niigata

(M. Mutsuro)

11) Nippon Atomic Industry Group Co., Ltd.

Nuclear Research Laboratory / 250 Suehiro-cho, Kawasaki-shi, Kanagawa

(S. Iijima, N. Kawai)

12) Osaka University

a) Faculty of Engineering / Yamadaue, Suita-shi, Osaka

(T. Sekiya)

b) Faculty of Science / 1-1, Machikaneyama, Toyonaka-shi, Osaka

(T. Wakatsuki, M. Muraoka)

13) Radiation Center of Osaka Prefecture

Shinya-cho, Sakai-shi, Osaka

(T. Azuma)

14) Rikkyo (St. Paul's) University

a) Department of Physics / 3, Ikebukuro, Toshima-ku, Tokyo

(I. Ogawa)

b) Institute for Atomic Energy / 2-5-1, Nagasaka, Yokosuka-shi, Kanagawa
(M. Hattori)

15) The Institute of Physical and Chemical Research
2-1, Hirosawa, Wako-shi, Saitama
(H. Kamitsubo)

16) Tohoku University

a) Faculty of Science /2-1-1 Katahira-cho, Sendai-shi, Miyagi
(S. Morita)

b) Laboratory of Nuclear Science / 1 Tomisawa, Kanayama, Sendai-shi, Miyagi
(M. Kimura)

17) Tokai University
Faculty of Engineering / 2-28-4 Tomigaya, Shibuya-ku, Tokyo
(Y. Kuroda)

18) Tokyo Institute of Technology

a) Faculty of Science / 2-12-1 Ohokayama, Meguro-ku, Tokyo
(Y. Oda, H. Taketani)

b) Research Laboratory of Nuclear Reactor / 2-12-1 Ohokayama, Meguro-ku, Tokyo
(N. Yamamuro)

19) Tokyo University of Education
Faculty of Science / 3-29-1 Ohtsuka, Bunkyo-ku, Tokyo
(J. Sanada, K. Katori)

20) University of Tokyo

a) Faculty of Science / 7-3-1 Hongo, Bunkyo-ku, Tokyo
(Y. Nogami)

b) Institute for Nuclear Study / 3-2-1 Midori-cho, Tanashi, Tokyo
(Y. Ishizaki, M. Sakai)

c) College of General Education / 865 Komaba, Meguro-ku, Tokyo
(T. Terasawa)

21) Waseda University
Department of Applied Physics / 17 Kikui-cho, Shinjuku-ku, Tokyo
(M. Yamada)

CONTENTS

CONTENTS OF THE JAPANESE PROGRESS REPORT INDC(JAP)13L (=EANDC(J)26L), August 1972

ELEMENT S A	QUANTITY	TYPE	ENERGY MIN	ENERGY MAX	DOCUMENTATION REF VOL PAGE DATE	LAB	COMMENTS
LI 006	N,ALPHA	EVAL-PROG		5.0 5	EANDC(J)26L 28 8/72	JAE	NAKAGAWA+.NDG
BE	TOTAL XSECT	EXPT-PROG	THR		EANDC(J)26L 34 8/72	KTO	KANDA+. NDG
BE	TOTAL XSECT	EXPT-PROG	2.0-3	3.0-1	EANDC(J)26L 61 8/72	TIT	AIZAWA+.TRANS AT 23,300,500,700DEG-C
C	DIFF ELASTIC	EXPT-PROG	2.2 7		EANDC(J)26L 11 8/72	JAE	YAMANOUTI+.30DEG TO 155DEG.NDG
C	DIFF INELAST	EXPT-PROG	2.2 7		EANDC(J)26L 11 8/72	JAE	YAMANOUTI+.30DEG TO 155DEG.NDG
C 012	ELASTIC	THEO-PROG		4.4 6	EANDC(J)26L 73 8/72	TOK	MORI+.COUPLED CHANNEL METHOD
SI 028	INELAST GAMMA	EXPT-PROG	1.8 6	3.1 6	EANDC(J)26L 9 8/72	JAE	TANAKA+.VDG,TOF,H-FREE SCIN.NDG
S	DIFF ELASTIC	EXPT-PROG	2.2 7		EANDC(J)26L 11 8/72	JAE	YAMANOUTI+.30DEG TO 155DEG.NDG
S	DIFF INELASTIC	EXPT-PROG	2.2 7		EANDC(J)26L 11 8/72	JAE	YAMANOUTI+.30DEG TO 155DEG.NDG
TI 047	N,PROTON	EXPT-PROG	3.4 6	5.0 6	EANDC(J)26L 16 8/72	JAE	GOTOH+.PRELIMINARY SIG BY ACTIVATION
FE	DIFF ELASTIC	THEO-PROG	1.4 6	3.3 6	EANDC(J)26L 11 8/72	JAE	TANAKA.COUPLED-CHANNEL AND OPTMDL
FE 054	N,PROTON	EXPT-PROG	1.7 6		EANDC(J)26L 17 8/72	JAE	GOTOH.10+-10MILLIBARN BY ACTIVATION
FE 056	DIFF INELAST	THEO-PROG	1.4 6	3.3 6	EANDC(J)26L 11 8/72	JAE	TANAKA.COUPLED-CHANNEL AND OPTMDL
FE 056	INELAST GAMMA	EXPT-PROG	8.5 5	2.0 6	EANDC(J)26L 9 8/72	JAE	TANAKA+.VDG,TOF,H-FREE SCIN.SPECT
NI	DIFF ELASTIC	THEO-PROG	2.0 6	3.0 6	EANDC(J)26L 11 8/72	JAE	TANAKA.COUPLED-CHANNEL AND OPTMDL
NI 058	DIFF INELAST	THEO-PROG	2.0 6	3.0 6	EANDC(J)26L 11 8/72	JAE	TANAKA.COUPLED-CHANNEL AND OPTMDL
ZN	DIFF ELASTIC	THEO-PROG	1.7 6	8.0 6	EANDC(J)26L 11 8/72	JAE	TANAKA.COUPLED-CHANNEL AND OPTMDL
ZN	DIFF INELAST	THEO-PROG	1.7 6	8.0 6	EANDC(J)26L 11 8/72	JAE	TANAKA.COUPLED-CHANNEL AND OPTMDL
ZR 090	N2N REACTION	EXPT-PROG	1.3 7	1.5 7	EANDC(J)26L 50 8/72	KYU	KANDA.PUBLISHED TO NP A185 177
MO 092	N2N REACTION	EXPT-PROG	1.3 7	1.5 7	EANDC(J)26L 50 8/72	KYU	KANDA.PUBLISHED TO NP A185 177
MO 092	N,PROTON	EXPT-PROG	1.3 7	1.5 7	EANDC(J)26L 50 8/72	KYU	KANDA.PUBLISHED TO NP A185 177
MO 092	N,ALPHA	EXPT-PROG	1.3 7	1.5 7	EANDC(J)26L 50 8/72	KYU	KANDA.PUBLISHED TO NP A185 177
PD	RESON PARAMS	EXPT-PROG	1.0 1	3.0 2	EANDC(J)26L 58 8/72	TIT	YAMAMURO+.TOF,AREA ANAL. IN TABLE
IN 115	TOT INELASTC	EXPT-PROG	3.4 6	4.9 4	EANDC(J)26L 36 8/72	KTO	KOBAYASHI+.TO ISOM,R-P COUNTER,FIGS
SN 120	DIFF ELASTIC	EXPT-PROG	1.5 6	3.5 6	EANDC(J)26L 6 8/72	JAE	TANAKA+.PAPER FOR 1972 BUDAPEST CONF
SN 120	DIFF INELAST	EXPT-PROG	1.5 6	3.5 6	EANDC(J)26L 6 8/72	JAE	TANAKA+.PAPER FOR 1972 BUDAPEST CONF
SN 120	INELAST GAMMA	EXPT-PROG	2.0 6	3.1 6	EANDC(J)26L 15 8/72	JAE	KIKUCHI+.TOF,SSD.GS ANGDIST.NDG
CS 141	FISS PROD GS	EXPT-PROG	NDG		EANDC(J)26L 47 8/72	KTO	TAMAI+.SPECTRUM IN FIG
GD	DIFF ELASTIC	EXPT-PROG	1.5 6	3.5 6	EANDC(J)26L 6 8/72	JAE	TANAKA+.PAPER FOR 1972 BUDAPEST CONF
GD	DIFF INELAST	EXPT-PROG	1.5 6	3.5 6	EANDC(J)26L 6 8/72	JAE	TANAKA+.PAPER FOR 1972 BUDAPEST CONF
RE 185	RESON PARAMS	EXPT-PROG		1.2 2	EANDC(J)26L 5 8/72	JAE	IDENO+.PUBLISHED IN NST 9(1972)261
RE 187	RESON PARAMS	EXPT-PROG		1.2 2	EANDC(J)26L 5 8/72	JAE	IDENO+.PUBLISHED IN NST 9(1972)261
PB	TOTAL XSECT	EXPT-PROG	1.5-3	3.0-2	EANDC(J)26L 34 8/72	KTO	KANDA+. IN FIG
TH 232	FISSION	EXPT-PROG	PILE		EANDC(J)26L 39 8/72	KTO	KOBAYASHI+.CFD C OTHER DATA IN TABLE
U 233	FISS YIELD	EXPT-PROG	THR		EANDC(J)26L 22 8/72	JAE	UMEZAWA.SUBMITTED TO JIN.PM-148
U 235	TOTAL XSECT	THEO-PROG	0	3.0 3	EANDC(J)26L 56 8/72	OSA	KITAZOE+.TBP IN AKE
U 238	N2N REACTION	EXPT-PROG	1.5 7		EANDC(J)26L 18 8/72	JAE	TAKEKOSHI+.SEARCH FOR FISSION-ISOMER
NP 237	N2N REACTION	EXPT-PROG	1.5 7		EANDC(J)26L 18 8/72	JAE	TAKEKOSHI+.SEARCH FOR FISSION-ISOMER
NP 237	FISSION	EXPT-PROG	PILE		EANDC(J)26L 39 8/72	KTO	KOBAYASHI+.CFD C OTHER DATA IN TABLE
NP 237	FISSION	EXPT-PROG	4.3 6	4.8 6	EANDC(J)26L 39 8/72	KTO	KOBAYASHI+.CFD C OTHER DATA IN FIG
AM 241	FISS YIELD	EXPT-PROG	THR		EANDC(J)26L 49 8/72	KTO	NAKAHARA+.PUBLISHED TO JIN 33 3239
CF 252	FRAG SPECTRA	EXPT-PROG	SPON		EANDC(J)26L 51 8/72	KYU	TSUJI+.E AND ANG DIST. IN FIGS
MANY	TOTAL XSECT	EVAL-PROG	NDG		EANDC(J)26L 30 8/72	JAE	KAWAI+.OPT-MDL CALC. IN FIGS
MANY	DIFF ELASTIC	EVAL-PROG	NDG		EANDC(J)26L 30 8/72	JAE	KAWAI+.OPT-MDL CALC. NDG
MANY	TOT INELASTC	EVAL-PROG	NDG		EANDC(J)26L 30 8/72	JAE	KAWAI+.SIMPLE MDL.RESULT IN FIGS
MANY	THRMLSCATLAW	THEO-PROG	THR		EANDC(J)26L 25 8/72	JAE	NAKAHARA.SUBMITTED TO NST
MANY	THRMLSCATLAW	THEO-PROG	THR		EANDC(J)26L 56 8/72	OSA	SEKIYA+.TBP IN TECH.REPORT OSAKA U.
MANY	N,GAMMA	THEO-PROG			EANDC(J)26L 54 8/72	OSA	MATSUOKA+.(N-Z)DEPENDENCE
BEO	TOT XSECT	EXPT-PROG	THR		EANDC(J)26L 34 8/72	KTO	KANDA+.NDG

I. Japan Atomic Energy Research Institute

A. Neutron Experiments-Linac

I-A-1. Electron Linear Accelerator

JAERI Linac Laboratory*

The construction of the new JAERI Linac, a 120-MeV s-band electron linear accelerator of which outline was described in EANDC(J) 22L, pp.1 - 2 (1971), was completed in April 1972, and is now at the final stage of the test operation. The specifications are as follows:

Frequency: 2856.75 MHz

Accelerating Tube: 5 sections with one klystron each

Section Nos. 1 and 2: Constant Impedance, Mode $2\pi/3$, Length 2m

Section Nos. 3 to 5: Constant Gradient, Mode $2\pi/3$, Length 3m

Power Rating: peak 20 MW (mean 20 kW) each

No load Beam Energy: 190 MeV

Pulse Width of the Beam: 5 nsec to 2 μsec

Peak Beam Current (presently achieved value):

250 mA with 0.1 μsec pulse width at 150 MeV

Schematic diagrams to show the arrangement of the linac facility are given in Figs. 1 and 2. A block diagram of the data acquisition and reduction system is shown in Fig. 3, in which an outline of the specifications

---

* H. Takekoshi, T. Fuketa, A. Asami, T. Tamura, N. Shikazono, Z. Matsumoto, Y. Kawarasaki, K. Mashiko, M. Ohkubo, Y. Nakajima, Y. Nobusaka, N. Akiyama, T. Shoji, M. Kitajima, M. Mizumoto, and K. Sakurai took part in the construction of the Linac.

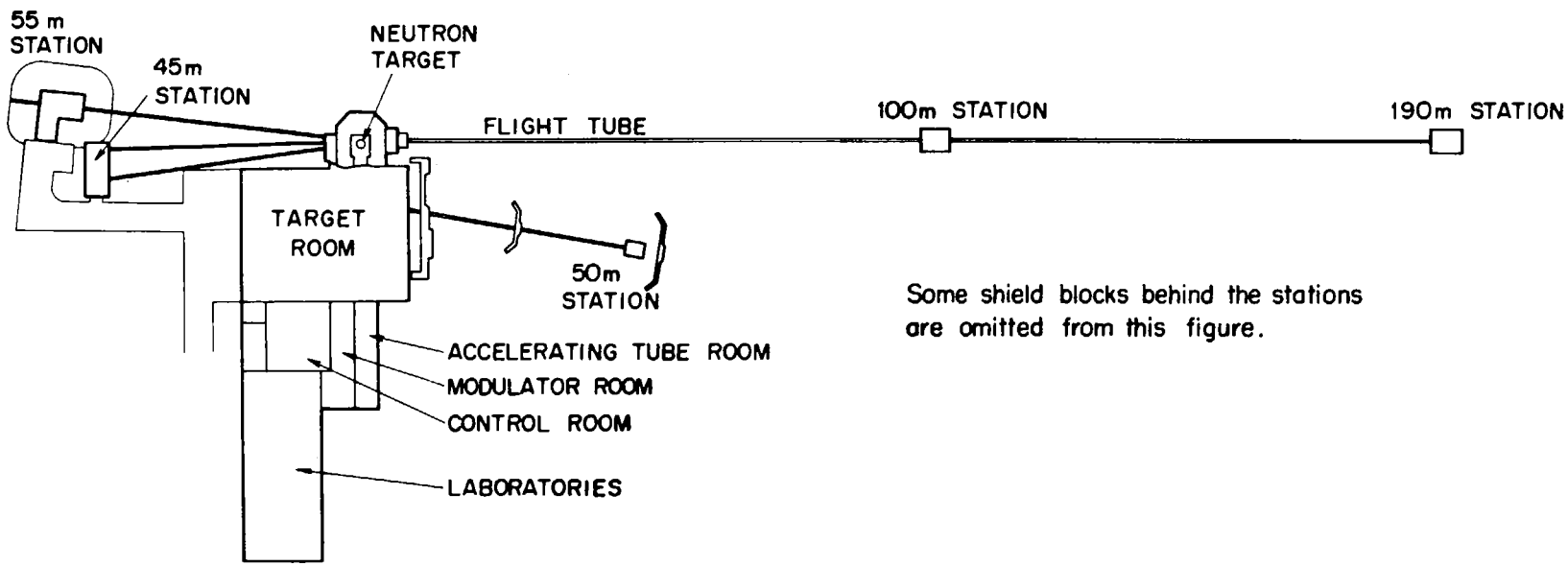

Fig. 1. Arrangement of the linac and the neutron flight paths.
Some shorter paths are omitted from the figure.

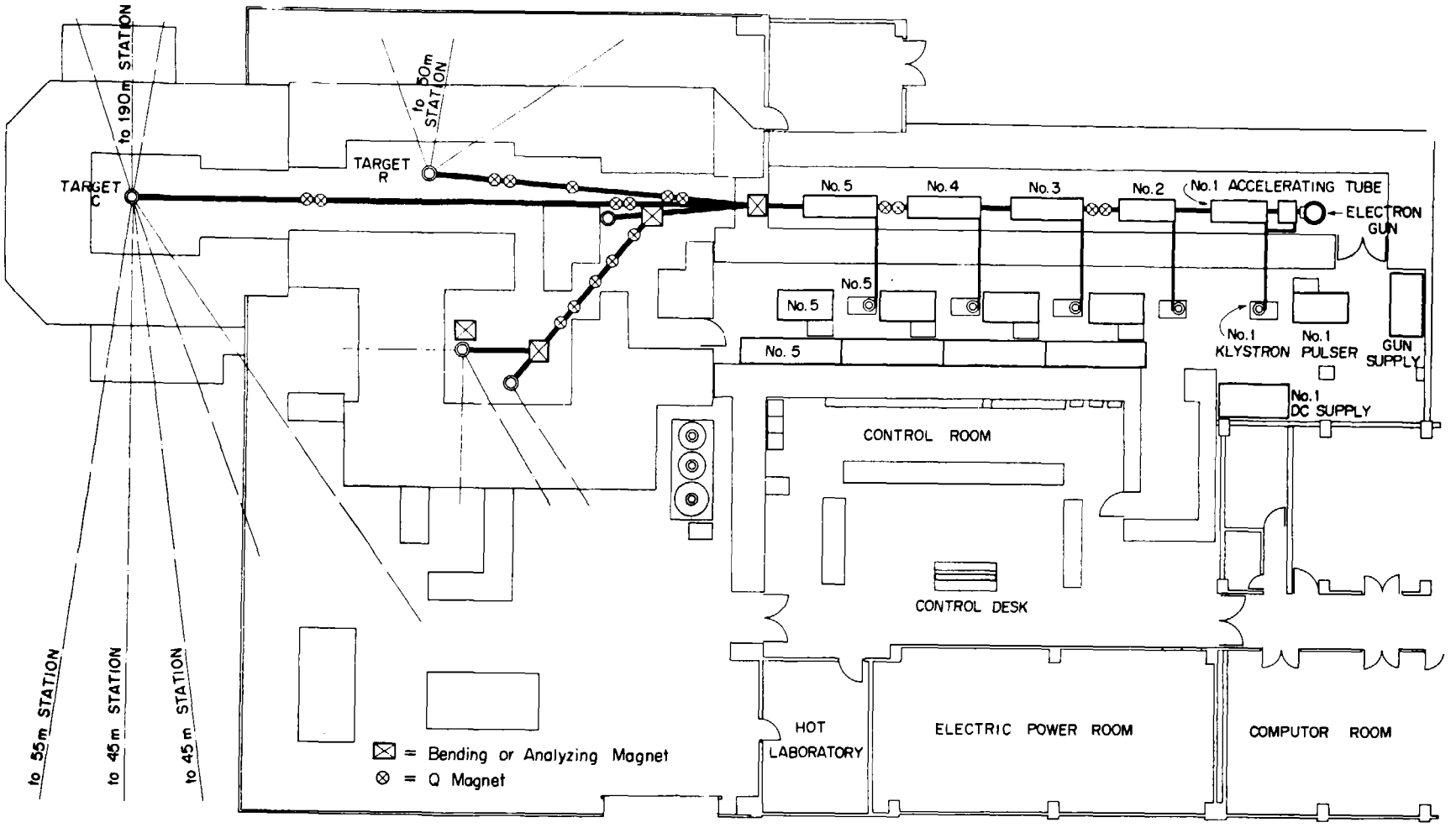

Fig. 2. Arrangement of the linac in the building.

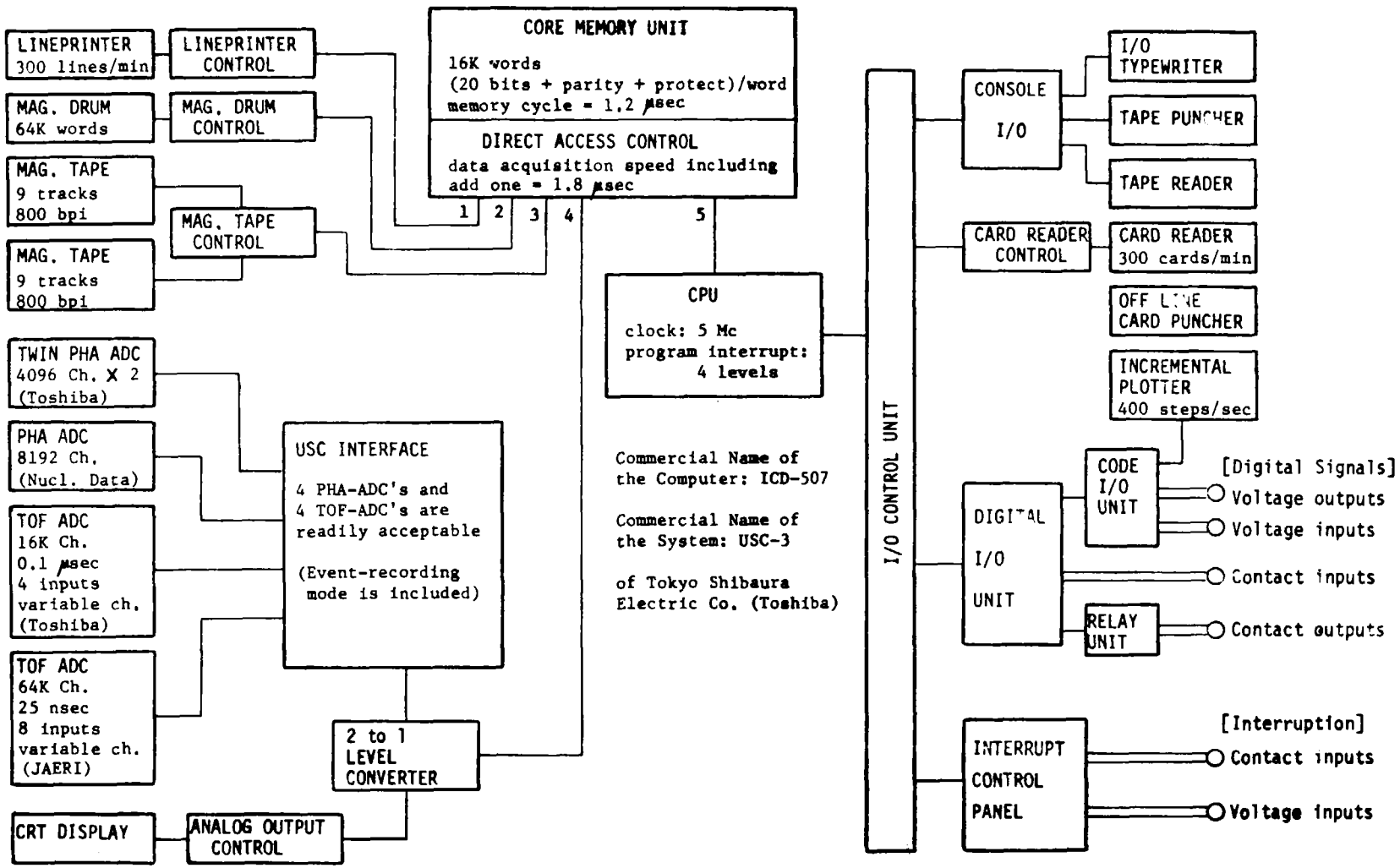

Fig. 3. JAERI Linac Experimental Data Acquisition and Reduction System (LEDARS).

is also given.

The first experiment on the neutron cross-section measurements will be the transmission measurements with a 190-m flight path. The neutron capture and scattering detector systems are now under preparation.

I-A-2. Slow Neutron Resonances of Rhenium

K. Ideno, T. Asami, Y. Nakajima, M. Ohkubo, and T. Fuketa

The result of neutron transmission measurements on rhenium with the former 20-MeV linac was published in J. Nucl. Sci. Technol., 9 (1972) 261 - 267 with an abstract as follows:

Neutron transmission measurements on natural rhenium were made in the energy region from 3 to 300 eV, using a LINAC neutron time-of-flight spectrometer. The resonance parameters of ^{185}Re and ^{187}Re were obtained below 120 eV by area and shape analyses based on the Breit-Wigner single level formula. Isotopic assignments of levels were taken from the data of other authors. The strength functions deduced are $(1.8 \pm 0.6) \times 10^{-4}$ for ^{185}Re and $(1.5 \pm 0.5) \times 10^{-4}$ for ^{187}Re. Correlations between level spacings were searched for and a series of equidistant levels was found in both nuclei.

B. Neutron Experiments-Van de Graaff Accelerator

I-B-1. Fast Neutron Scattering from ^{120}Sn and Gd

S. Tanaka, Y. Tomita, Y. Yamanouti and K. Ideno

The paper on this subject is submitted to "Conference on Nuclear Structure Study with Neutrons, Hungary, 1972". The abstract of this study is as follows:

The angular distributions of neutrons scattered from ^{120}Sn and natural Gd were measured in the energy range of 1.5 to 3.5 MeV with 500-keV steps. In order to get a good resolution especially for Gd spectra, the measurement was done by using a newly constructed multi-angle time-of-flight spectrometer with three detectors and with flight paths of 8 m.[1)]

The results were compared with calculations using both the spherical optical model and the coupled-channels theory. In the calculations, the optical potential form and its parameter values almost same as those in our previous work[2)] were used. The coupling parameters β_2 were taken as 0.112 for ^{120}Sn and 0.30 for Gd. As shown in figs. 1 and 2, the angular distributions calculated with the coupled-channels theory fit the experimental data better than those calculated with the spherical optical model.

The authors are greatly indebted for the use of a ^{120}Sn sample in the ORNL pool by the courtesy of EANDC and US AEC.

References:

1) Y. Yamanouti, to be published.

2) S. Tanaka, Y. Tomita, K. Ideno and S. Kikuchi, Nucl. Phys. A179 (1972) 513.

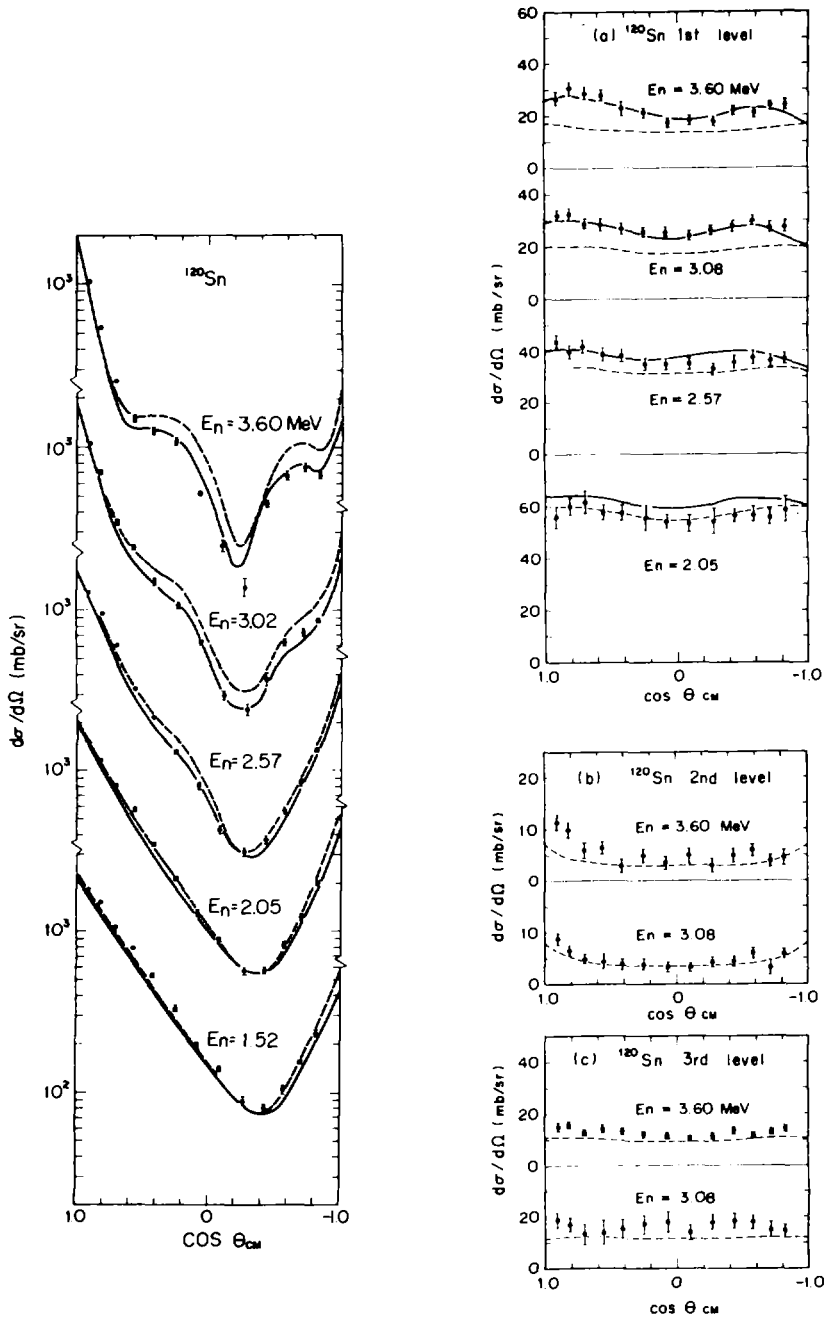

Fig. 1 Differential cross sections for elastic (left-hand side) and inelastic (right-hand side) scattering by ^{120}Sn. The closed points are the experimental data. The dashed and solid curves for the elastic scattering are cross sections calculated with the spherical optical potential and with the coupled-channels theory, respectively. The compound elastic cross sections calculated with the Moldauer theory were added to both the calculated results. The dashed curves for the inelastic scattering are cross sections calculated with the Moldauer theory. The solid curves represent the results of the coupled-channels theory plus those of the Moldauer theory.

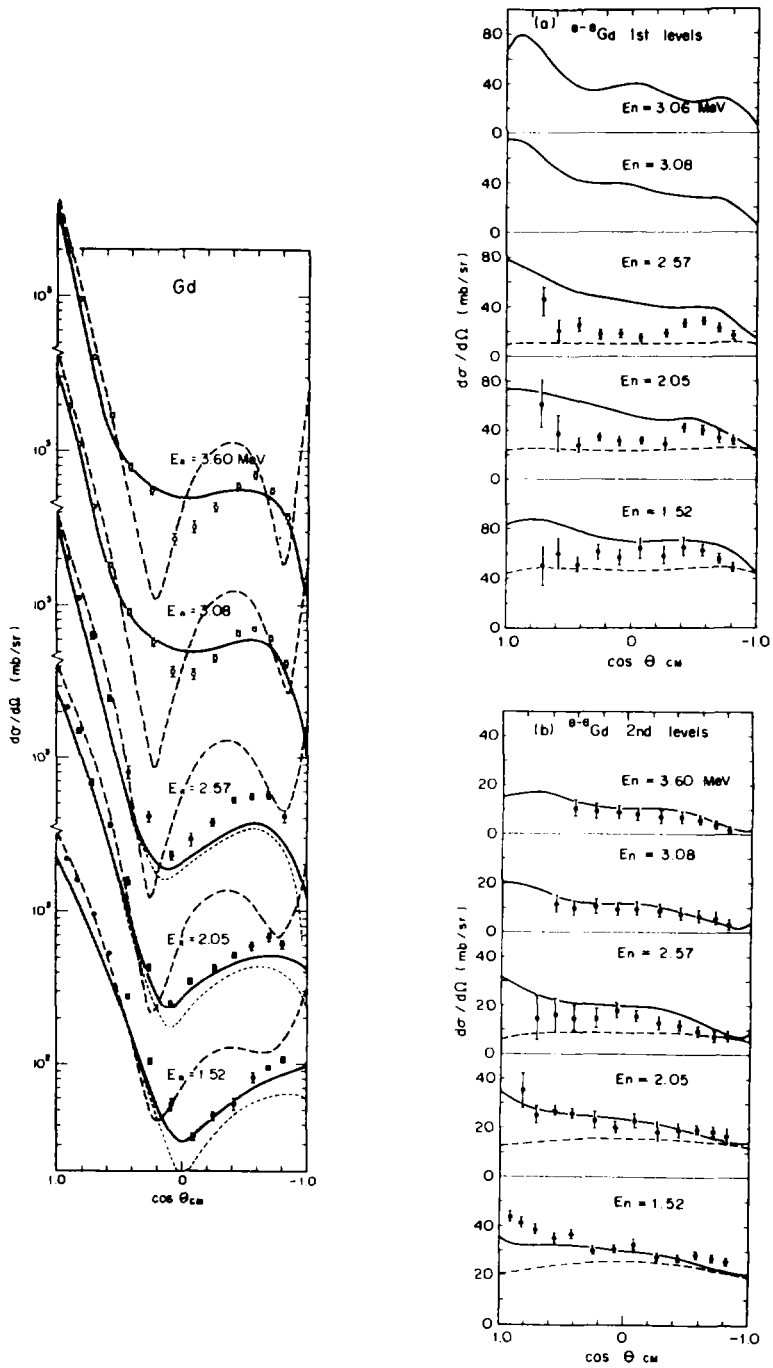

Fig. 2 Differential cross sections for elastic and inelastic scattering by gadolinium. The points are the experimental data. The open circles indicate the elastic plus the inelastic cross sections for the first 2^+ levels in gadolinium isotopes. Accordingly, the direct inelastic cross sections for these levels calculated with the coupled-channels theory were added to the elastic cross sections calculated with this theory. Excluding this case, the solid and dashed curves have the same meaning as in fig. 1. In order to show the contribution of the compound process, the results due only to the coupled-channels calculation are shown by dotted curves in the figure of left-hand side.

I-B-2. Preliminary Test for High Resolution Inelastic Cross Section Measurements

S. Tanaka, K. Ideno and T. Tonai*

A preliminary test for high resolution inelastic cross section measurements has been made by detecting the de-excitation gamma rays with a hydrogen-free carbon fluoride liquid scintillator (NE 226). The method is similar to what was initiated by Perey et al.[1] Neutrons with continuous spectra were produced at a thick Li target with bombardment of proton beams from the 5.5 MV Van de Graaff accelerator. Neutron energy was determined by the time-of-flight technique with a flight path of 9.38 m.

The purpose of the present test is to see to what extent the flight path can be elongated. Si and Fe samples were placed in the neutron beams, and the de-excitation gamma rays from the first excited states were cbserved. The neutron energies were covered from the threshold to 3.1 MeV for ^{28}Si, and from the threshold to 2.0 MeV for ^{56}Fe. The figure shows the time-of-flight spectrum for the inelastic scattering from ^{56}Fe. Numbers above peaks represent neutron energies. The data were acquired for a period of 1.2 hours. The resolution is estimated to be 1.7 ns using FWHM of the gamma-ray peak from the target.

Although rather a large sample was used for the present test, it was ascertained that the extention of the flight path up to, say, 30 m is possible.

Reference

1) F. G. Perey, W. E. Kinney and R. L. Macklin, Proc. of 3rd Conf.

---

* Dept. of Nuclear Engineering, Kyushu Univ., Fukuoka

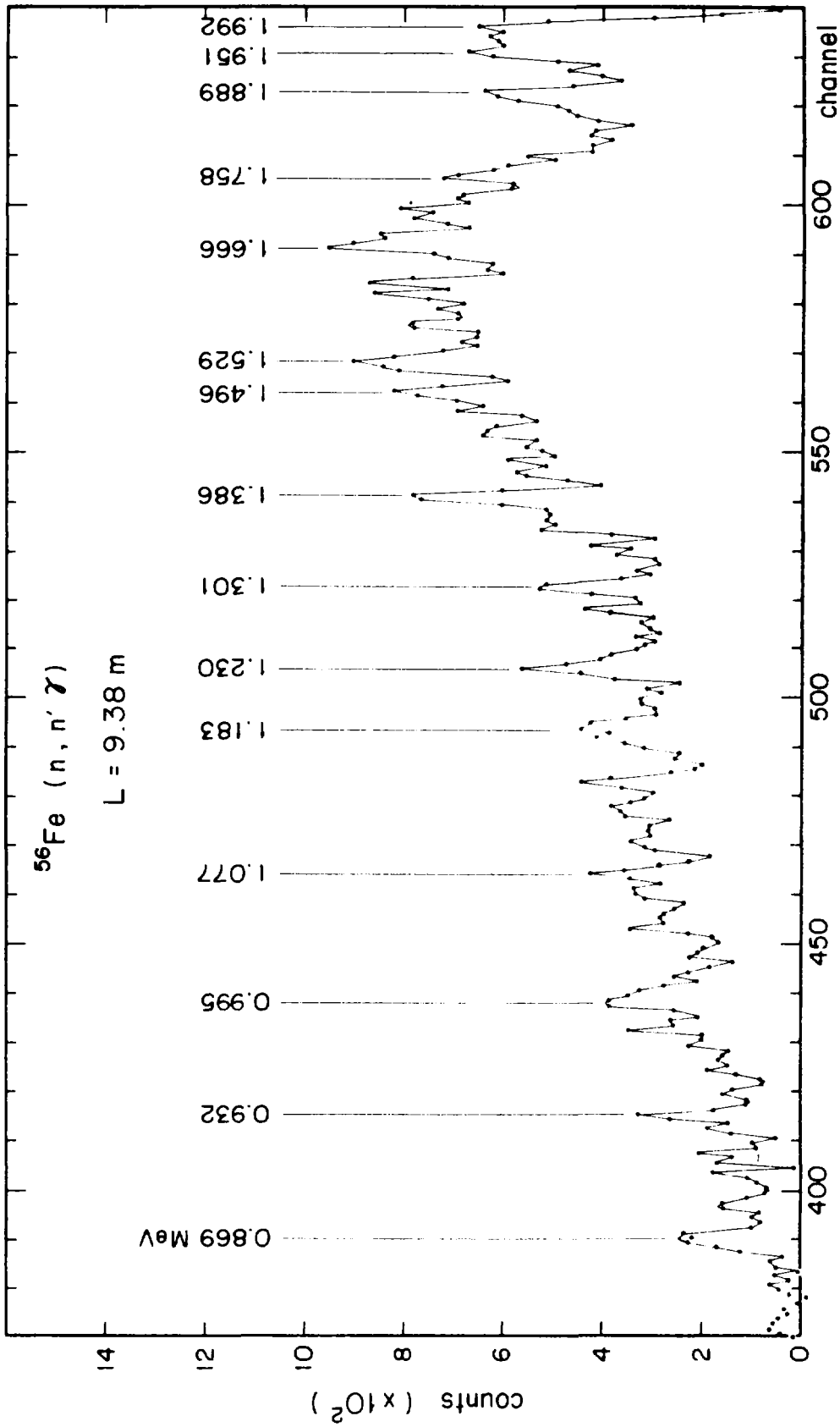
^{56}Fe (n, n' γ)
L = 9.38 m
0.869 MeV
0.932
0.995
1.077
1.183
1.230
1.301
1.386
1.496
1.529
1.666
1.758
1.889
1.951
1.992
counts (x10^2)
0
2
4
6
8
10
12
14
400
450
500
550
600
channel

"Neutron Cross Sections and Technology" (Knoxville). Vol. 1, p. 191 (1971).

I-B-3. Elastic and Inelastic Scattering of 21.5 MeV Neutrons from Carbon and Sulphur

Y. Yamanouti and S. Tanaka

The angular distributions of neutrons elastically and inelastically scattered from carbon and sulphur were measured at a neutron energy 21.5 MeV and at scattering angles from 30° to 155° by using a multi-angle time-of-flight spectrometer.

Data analysis is now in progress.

I-B-4. Analysis of Fast Neutron Scattering From Fe, Ni and Zn Using the Coupled-Channels Theory

S. Tanaka

The experimental data for the angular distributions of neutrons scattered from Fe, Ni and Zn were compared with calculations using both the spherical optical model and the coupled-channels theory. As for the experimental data, our previous data[1),2)] in the energy range of 1.37-3.26 MeV for Fe, 2.01-3.0 MeV for Ni and 1.71-7.99 MeV for Zn were used.

In the calculations, the values of optical parameters were taken the same as those used in ref. 3), except for the following two; r_0=1.23 fm instead of 1.25 fm, and V=51.5-0.3E-24.0(N-Z)/A instead of V=46.0 MeV. The value of V is consistent with that in ref. 3), if one takes into account

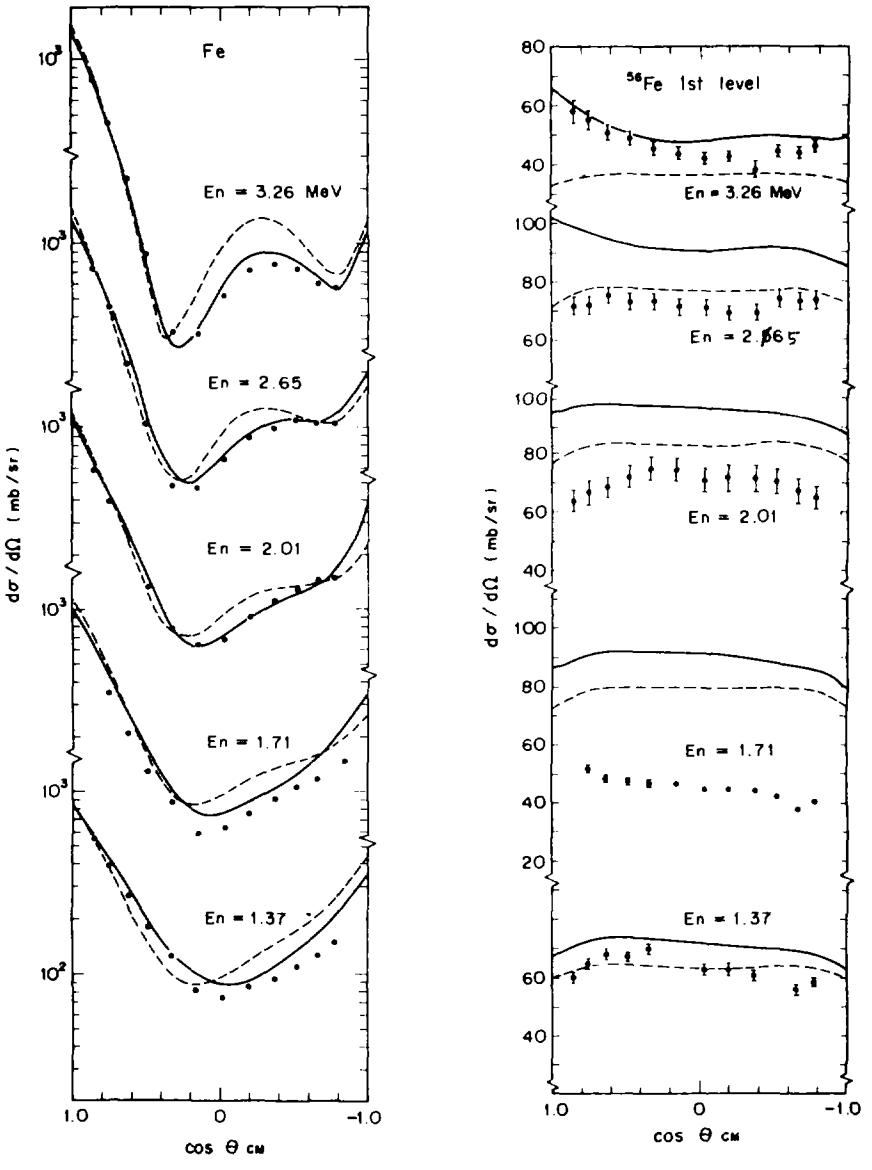

Fig. 1 Differential cross sections for elastic (left-hand side) and inelastic (right-hand side) scattering by iron. The closed points are our experimental data[1]. The dashed and solid curves for the elastic scattering are cross sections calculated with the spherical optical potential and with the coupled-channels theory, respectively. The compound elastic cross sections calculated with the Moldauer theory were added to both the calculated results. The dashed curves for the inelastic scattering are cross sections calculated with the Moldauer theory. The solid curves represent the results of the coupled-channels calculation plus those of the Moldauer theory.

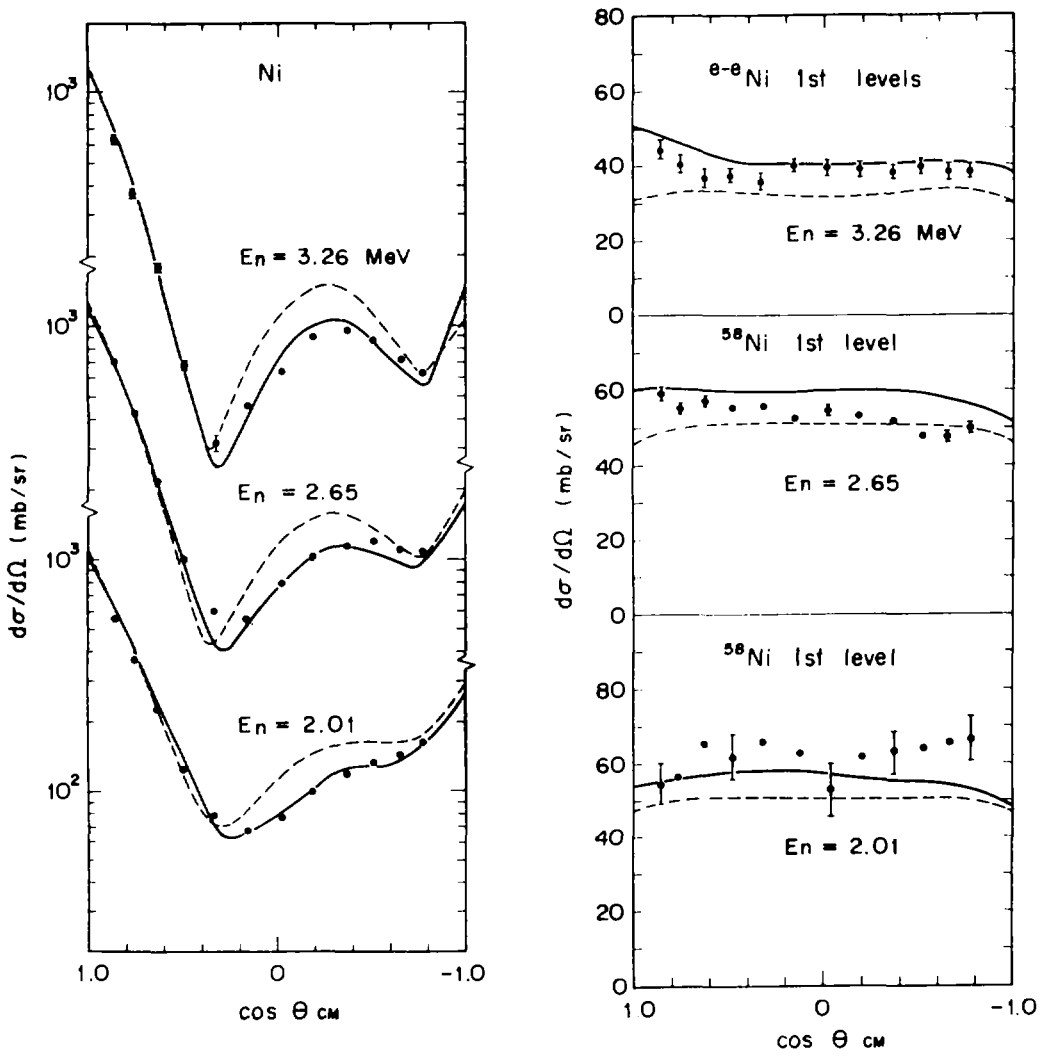

Fig. 2 Differential cross sections for elastic and inelastic scattering by nickel. The points[1] and curves have the same meaning as in fig. 1.

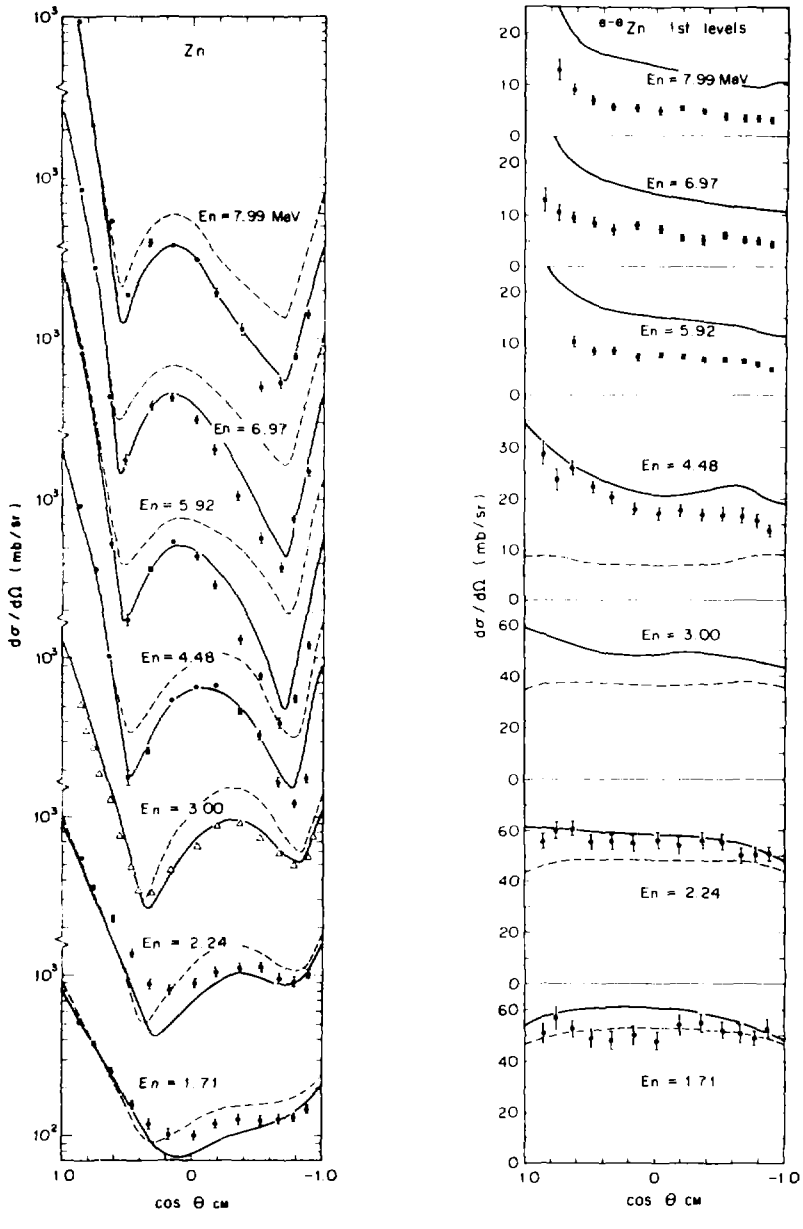

Fig. 3 Differential cross sections for elastic and inelastic scattering by zinc. The closed points are our experimental data[2]. The open triangles are data of Holmqvist and Wiedling[5]. The curves have the same meaning as in Fig. 1. The compound processes are neglected for the case of incident neutron energies higher than 5 MeV.

the energy-dependent term and the charge-symmetry term also for the value in ref. 3). In the coupled-channels calculations, complex couplings between the ground and the first excited levels were considered in a vibrational mode, and the values of β_2 were taken from ref. 4). As shown in figs. 1-3, the angular distributions of the elastic scattering calculated with the coupled-channels theory fit the observed data better than those calculated with the spherical optical model.

References:

1) K. Tsukada, S. Tanaka, Y. Tomita and M. Maruyama, Nucl. Phys. A125 (1969) 641.

2) S. Tanaka, K. Tsukada, M. Maruyama and Y. Tomita, "Nuclear Data for Reactors" (Helsinki Conf.) Vol. II, p.317 (1970).
K. Tsukada, S. Tanaka, Y. Tomita and M. Maruyama, "Nuclear Data for Reactors" (Helsinki Conf.) Vol. II, p.305 (1970).

3) S. Tanaka, Y. Tomita, K. Ideno and S. Kikuchi, Nucl. Phys. A179 (1972) 513.

4) P. H. Stelson and L. Grodzins, Nucl. Data Sect. A1 (1965) 21.

5) B. Holmqvist and T. Wiedling, AE-337 (1968).

I-B-5. Study of Energy Levels of ^{120}Sn through the (n, n'γ) Reaction

S. Kikuchi and Y. Sugiyama

The energy levels of ^{120}Sn were studied by means of the (n, n'γ) reaction in the energy range 2.0 ~ 3.1 MeV. A 20 cc Ge(Li) detector, associated with a pulsed-beam time-of-flight spectrometer, was used to detect γ-rays. From the threshold energies of γ-ray production cross

sections, the energies of levels were determined. For the purpose of obtaining informations about spins and parities of these levels, the γ-ray angular distributions were measured at E_n=2.3, 2.7 and 3.1 MeV. Detailed analysis is now in progress.

I-B-6. $^{47}Ti(n,p)^{47}Sc$ Cross Section

H. Gotoh, H. Yagi, I. Kimura* and K. Kobayashi*

The activation cross section for the $^{47}Ti(n,p)^{47}Sc$ reaction was measured in the neutron energy region from 3.37 to 5.01 MeV using the d-d neutrons from the 2.2 MeV JAERI Van de Graaff machine. The numbers of neutrons incident on the individual titanium samples were measured with a pair of semiconductor proton recoil counters. Each counter was composed of a polyethylene radiator and a silicon detector. One was used for the main neutron detector, and the other for the monitor.

On the way of analyzing neutron data, the authors derived several useful formulae for the response function, the sensitivity and the detection efficiency of the neutron detection system[1-2].

Two expressions in elementary functions were also obtained for the energy distribution of neutrons incident on circular targets[3]. These expressions are applicable to the neutrons from the reactions d-d, t-p, d-t, ^{7}Li-p, etc.

The activities of ^{47}Sc were determined by measuring gamma rays with an NaI(Tl) scintillator or a Ge(Li) detector. The detailed analysis of data are now in progress. The preliminary analysis shows that the cross

---

* Research Reactor Institute, Kyoto University.

sections are 15 to 20 mb lower than Ghorai et al's results[4] in the energy region from 4 to 5 MeV.

References:

1) H. Gotoh and H. Yagi, Nucl. Instr. Meth. 97 (1971) 419.

2) H. Gotoh and H. Yagi, Nucl. Instr. Meth. 101 (1972) 395.

3) H. Gotoh, H. Yagi and K. Kobayashi, Nucl. Instr. Meth. 100 (1972) 473.

4) S. K. Ghorai, J. R. Cooper, J. D. Moore and W. L. Alford, J. of Nuclear Energy 25 (1971) 319.

I-B-7. $^{54}Fe(n,p)^{54}Mn$ Cross Section

Hiroshi Gotoh

The activation cross section for the $^{54}Fe(n,p)^{54}Mn$ reaction was measured at the neutron energy of 1.7 MeV using t-p neutrons from the 3 MeV Van de Graaff accelerator of National Institute of Radiological Sciences. A natural iron pellet of about 7.8 gr was irradiated about 11 hours at a place 5 cm apart from the tritium metal target. The neutron flux at the place was counted using a semiconductor proton recoil counter with a 30 μ thick polyethylene radiator before the pellet irradiation. The gamma activity of ^{54}Mn was measured for 400 min (same for the background) with an NaI(Tl) (3 inch in diameter and 3 inch in height) scintillator at the low background cell in Mt. Nokogiri, Institute for Nuclear Study, University of Tokyo.

The result was 10 ± 10 mb at E_n = 1.7 MeV.

C. Others

I-C-1. Search for Fissioning Isomers of ^{236}Np and ^{237}U in the Region of Half-Lives over 60 μs

E. Takekoshi and Y. Tsukihashi

The search for fissioning isomer of ^{236}Np in the $^{237}Np(n, 2n)$ reaction with 14.8 MeV neutrons is presented in the region of half-lives from 7 μs to 1 min in the previous work[1]. As the results, the upper limit of $\sigma_{f,delayed}/\sigma_{f,prompt}$-value for ^{236}Np was estimated to be 1×10^{-5}. In the present work, further search for fissioning isomer of ^{236}Np was made in the region of half-lives over 60 μs. In comparison with the case of ^{236}Np, search for fissioning isomer of ^{237}U was also made. The experimental conditions were almost same as in the previous work, except the following. The method of pulsed operation for deuteron beams was improved from the system with one deflector to that with double deflectors, and the ratio of any residual beam intensity between bursts to the main beam intensity within a burst was reduced from 2×10^{-7} to 5×10^{-8}. The half-lives studied was in the regions from 60 μs to 1 min and of 1 hr. The fission chambers used* were characterized by the thickness and the active area of samples; i.e. for ^{237}Np 300 $\mu g.cm^{-2}$ and 2.5 cmØ x 5 cm, and for ^{238}U (depleted to 0.046% for ^{235}U) 1 $mg.cm^{-2}$ and 2.5 cmØ x 8.1 cm. The $\sigma_{f,delayed}/\sigma_{f,prompt}$-value for each pulse operation mode was shown in fig. 1. The upper limits for these values in the region from 60 μs to 1 min for ^{236}Np and ^{237}U fissioning isomers were estimated to be 1×10^{-6} within the deviations from the average value of 2×10^{-6}, which may be attributed to the conditions of

* The fission chamber were manufactured by the 20th Century Electronics LTD in the U.K.

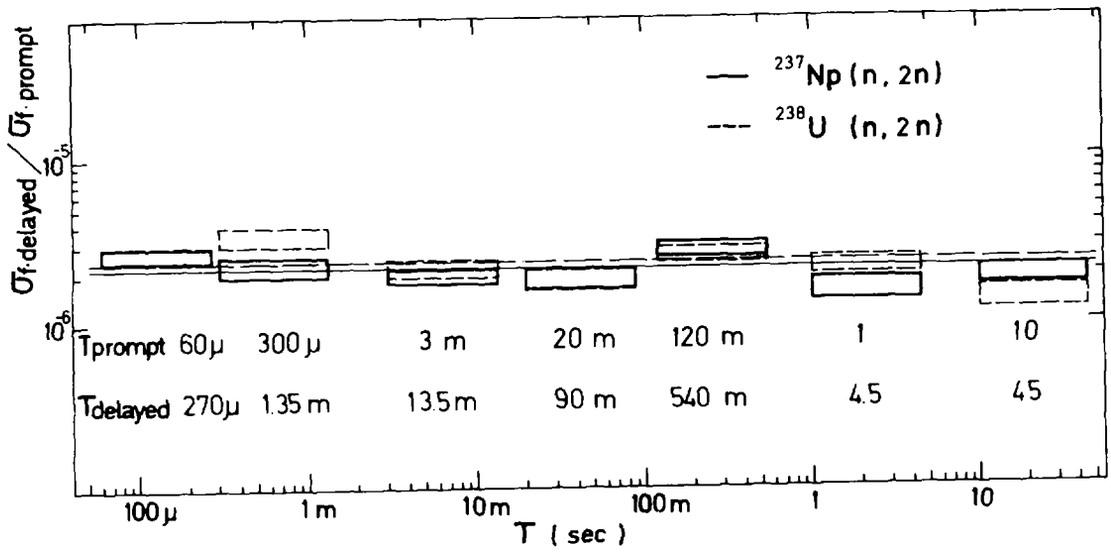

Fig. 1. $\sigma_{f,delayed}/\sigma_{f,prompt}$-values as a function of each pulse mode. T_{prompt} and $T_{delayed}$ mean the pulse duration and the time interval for measurement after beam pulse, respectively.

pulse neutrons. The upper limits were also estimated to be $(2.1\pm1.0) \times 10^{-8}$ for ^{236}Np and $(3.8\pm1.0) \times 10^{-7}$ for ^{237}U, under the irradiation of 1 hr.

References

1) E. Takekoshi, J. Phys. Soc. Japan 30 (1971) 284.

I-C-2. Gamma Decay Probability of Excited Oblate (or prolate) and Fissioning Isomeric States

T. Takemasa*, M. Wakai*, M. Sano* and E. Takekoshi

The possibility of existence of oblate (or prolate) shape-isomers is explored for even nuclei in the neutron-deficient nuclei with Z ~ 50, N ~ 82 and the rare-earth nuclei. It is found that the theoretical B(E2) values between oblate and prolate states are much hindered compared with those of the first 2^+ states. In the cases of the rare-earth, however, the theoretical values of the excitation energies of oblate states are very large, and the calculated half-lives of such oblate states becomes shorter than those of the first 2^+ states. The gamma decay of the fissioning isomers are also calculated. On the assumption of a pure configuration for fissioning isomer state, it is obtained that the calculated half-lives for the gamma decay are much longer than the measured values for the fission of the isomeric state. The method of calculation and the calculated B(E2) values between oblate and prolate states are summarized in the reference 1. The calculated B(E2) values between rotational bands in the ground and the fissioning isomeric states are shown in Fig. 1.

* Department of Physics, Osaka University

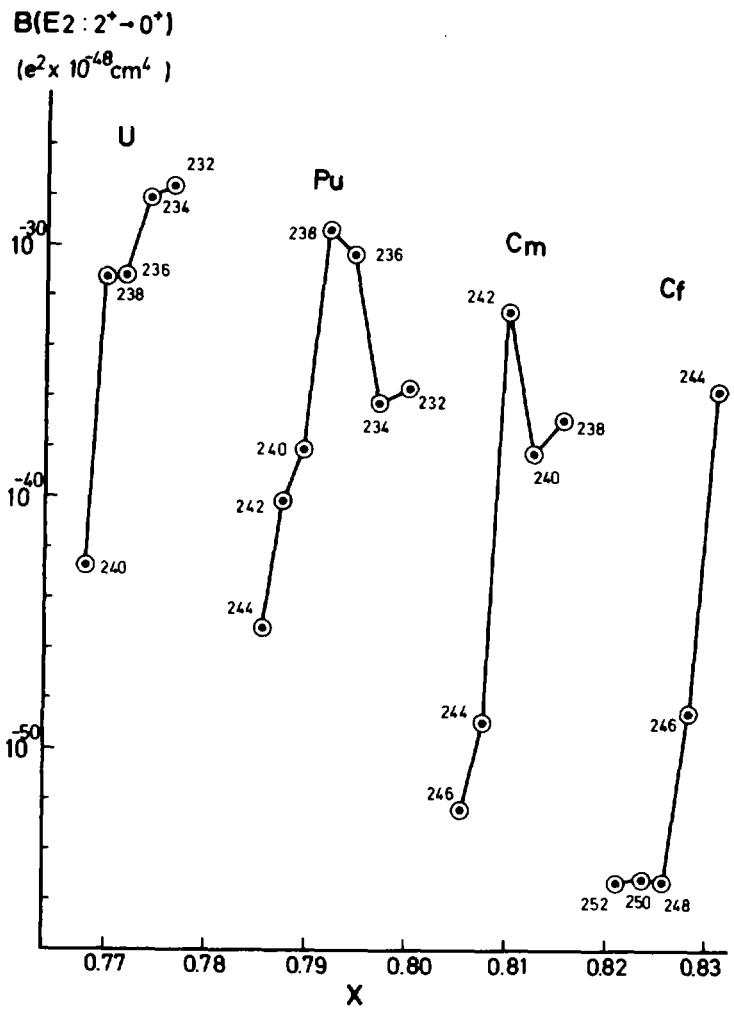

Fig. 1. The calculated B(E2) values from 2^+ state of rotational band in the fissioning isomer to 0^+ state of rotational band in the ground state as a function of fissility parameter X, which is calculated from mass formula by W.D. Myers and W.J. Swiatecki (Arkiv for Physik 36 (1967) 343). The deformation parameters, ε and ε_4, of intrinsic wave functions for the fissioning isomeric state and the ground state are taken from UCRL-18899 (1969) by C.F. Tsang.

Reference

1) M. Muraoka, T. Takemasa, M. Wakai and E. Takekoshi, JAERI Report 1221 (1972) p.94 (in Japanese)

I-C-3. Independent Isomeric Yield Ratio of ^{148}Pm in the Thermal-Neutron Induced Fission of ^{233}U

H. Umezawa

A paper on this subject was submitted to the J. Inorg. Nucl. Chem. with an abstract as follows:

Fractional independent yields of 41.3-d ^{148m}Pm (6-) and 5.37-d ^{148g}Pm (1-) have been determined in the thermal-neutron induced fission of ^{233}U by radiochemical techniques. Calculation based on a statistical theory of the spin distribution of the primary fragment has been made for the isomer ratio. A value of mean angular momentum of the primary fragment, $\bar{J} = 8.3 \pm 2.0\ \hbar$, was obtained by comparing the experimental isomer ratio, $\sigma_m/(\sigma_m+\sigma_g) = 0.80 \pm 0.06$, with the calculated values. The magnitude of the fragment angular momentum agreed well with a predicted value resulting from calculation based on the statistical model using the fragment excitation energy which has been estimated from the experimental data of the prompt neutron and gamma-ray emissions.

I-C-4. Decay of ^{95}Zr

T. Suzuki, Y. Nakahara and H. Umezawa

Decay and growth of γ rays emitting from a ^{95}Zr source which was prepared soon after separating from the daughter, ^{95}Nb, were followed for about 100 days with a Ge(Li) detector.

The half-life of ^{95}Zr was found to be 63.6 days which is slightly shorter than the literature values, while the observed half-life of ^{95}Nb agreed well with the reported values. The emission probabilities of the γ rays of 724.2 keV and of 756.7 keV per disintegration of ^{95}Zr were determined to be 43.9 ± 0.4% and 54.4 ± 0.5%, respectively, which agreed with the recent results obtained by other workers[1,2] within the experimental errors.

References:

1) C. Foin, J. Oms, J. Blachot et J. Crancon, Nucl. Phys., A123 (1969) 513.
2) S. M. Brahmavar and J. H. Hamilton, Phys. Rev., 187 (1969) 1487.

I-C-5. Nuclear Resonance Scattering from Tin using Thermal-Neutron-Capture Gamma-Rays in Lead

Y. Kawarasaki

Re-measurement of the nuclear resonance scattering from natural tin using thermal-neutron-capture gamma-ray in natural lead[1] was carried out by means of an improved measurement system[2].

A whole measurement contains; 1) temperature variation of the tin scatterer from 18°C to 418°C by a step of 50°C, 2) angular distribution of

the elastic peak at the angles of 90° to 135°, 3) transmission of the incident gamma-ray with the tin absorber of thickness up to 210 mm, and 4) search of inelastic and/or cascade lines in much closer geometry.

From the result of the angular distribution measurement which shows the spin sequence of 0-1-0 and the presence of the cascade gamma-ray of 1171 keV, it is found that the isotope responsible for the resonance scattering should be Sn-120.

From the result of the transmission measurement, it is found that the resonance level is excited by the capture gamma-ray of 6731 keV following neutron capture in Pb-204[3].

Further analysis for level width and energy of separation, and effective scattering cross-section is now in progress.

References;

1) N. Shikazono & Y. Kawarasaki, J. Phys. Soc. Japan 26 (1969) 1319.

2) Y. Kawarasaki, to be published in Nucl. Instr. Methods.

3) E. T. Jurney, H. T. Motz & S. H. Vegors; Nucl. Phys. A94 (1967) 351.

I-C-6. Study of odd-A nuclei in the 2s-1d shell by means of the (γ, γ') reaction

N. Shikazono and Y. Kawarasaki

The result of resonant scattering of photons from odd-A nuclei in the 2s-1d shell with the former 20 MeV linac was published in Nucl. Phys. A188 (1972) 461 with an abstract as follows:

Bremsstrahlung produced by electrons from the linac was used as a γ-ray source and a Ge(Li) detector was used to detect the resonantly

scattered γ rays. The scatterers used were; ^{19}F, ^{23}Na, ^{27}Al, ^{31}P, ^{35}Cl and ^{39}K. For ^{19}F, ^{23}Na, ^{27}Al and ^{31}P, many γ-rays were observed in contrast to the results for ^{35}Cl and ^{39}K. The results were compared with 180° inelastic electron scattering data from which one can conclude that most of the observed γ-rays have M1 character. Transitions from some T = 3/2 states were found and the transition strengths and the decay properties of these states are discussed.

I-C-7. Interpolation Formula of Thermal Neutron Scattering Law in Temperature Interval

Y. Nakahara

A paper on this subject is submitted to J. Nucl. Sci. Technol.

A very useful formula to interpolate thermal neutron scattering law in the temperature interval is derived by dividing the scattering law into two parts strongly and weakly dependent on temperature. The strong temperature dependence of the scattering law is characterized by Debye-Waller factors which are found to increase almost linearly with temperature for most of moderators. The Debye-Waller factor is approximated by a linear function of temperature with the proportional constant determined so as to give the exact scattering laws at boundaries of the temperature interval. The interpolation formula finally obtained to get the scattering law $S(\alpha, \beta)$ at T in the interval $[T_1, T_2]$ from the values of $S(\alpha, \beta)$ at T_1 and T_2 is

$$S(\alpha, \beta, T) = \frac{T}{T_1}\left[\frac{T_2 S(\alpha, \beta, T_1)}{T_1 S(\alpha, \beta, T_2)}\right]^{-\left(\frac{T - T_1}{T_2 - T_1}\right)} S(\alpha, \beta, T_1).$$

In order to make sure of the usefulness and accuracy of this formula we applied it to two typical moderators: graphite and light water. For example, some results of our calculation are shown in Figure. We used the GASKET/J code[1),2)] to obtain reference data of $S(\alpha, \beta)$. In the case of light water the interpolation was performed in the interval 100°C, 200°C to get $S(\alpha, \beta)$ at 150°C. Comparisons between Haywood's experimental data, the GASKET/J and interpolated values are made in Fig. Agreements between them are quite good.

It has been found that interpolated values are accurate within experimental errors in the practical range of (α, β) for graphite and light water.

Our formula is very simple and requires only a very short time of computation. With the aid of it numerical sets of $S(\alpha, \beta)$ at any practical temperature may be easily obtained with satisfactory accuracy from the ENDF.

References

1) J. U. Koppel, J. R. Triplett and Y. D. Naliboff, GA-7417 (1967).

2) Y. Nakahara and S. Ayao, JAERI-memo 3514 (1969) (unpublished).

3) B. C. Haywood, AERE-R 4484 (1964).

4) H. C. Honeck, BNL-8381 (1965).

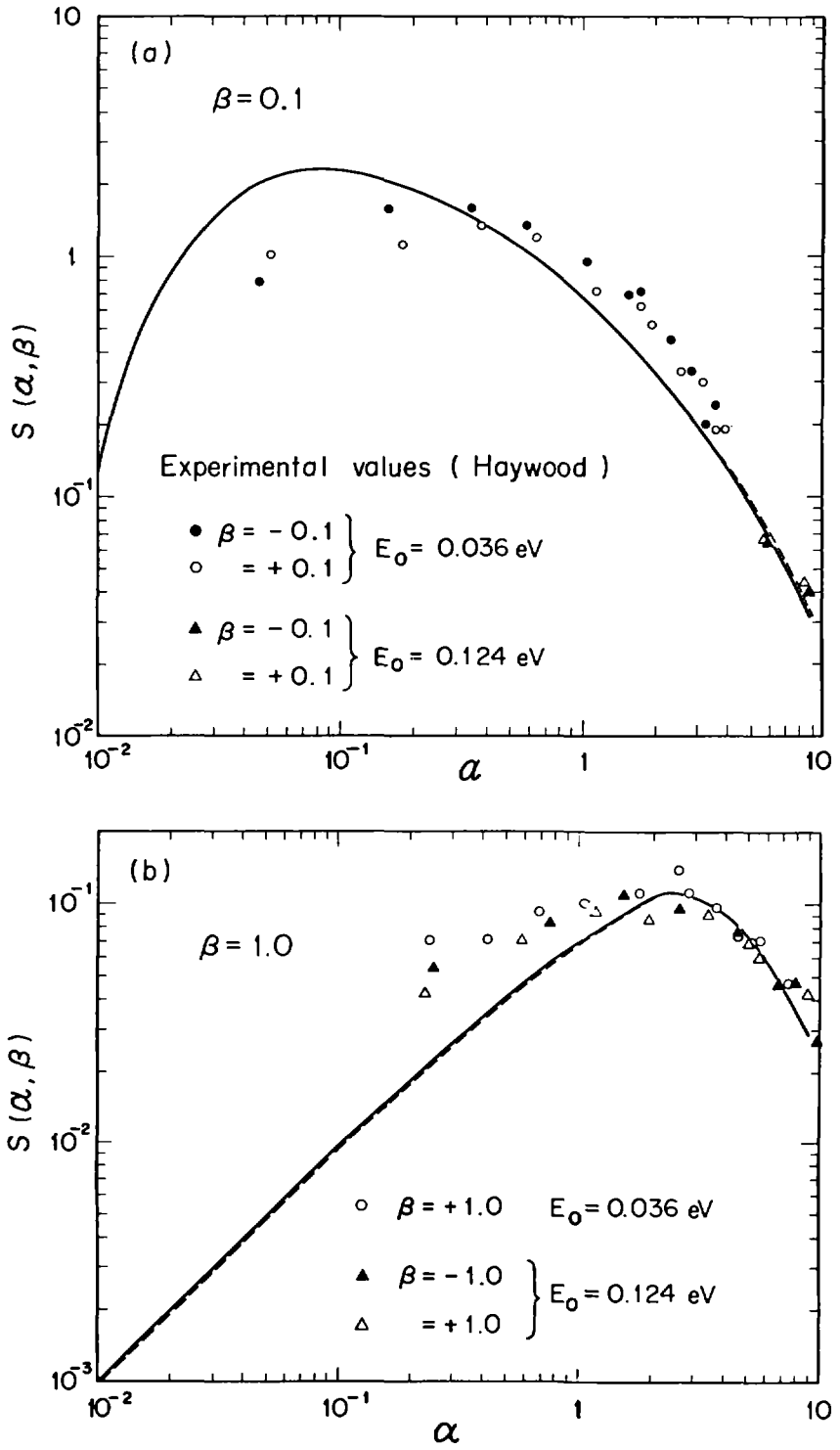

Scattering law for light water at 150°C

——— Results of the GASKET/J calculation,

----- Approximate values interpolated from $S(\alpha, \beta)$ at 100 and 200°C.

D. Japanese Nuclear Data Committee

I-D-1. Analysis of $^{6}Li(n,\alpha)T$ Reaction Cross Section

T. Nakagawa, S. Igarasi and K. Okamoto*

The cross section of $^{6}Li(n,\alpha)T$ up to 500 keV is analysed with some kinds of cross-section formulae. The cross-section curve of $^{6}Li(n,\alpha)T$ is usually described by a characteristic formula including two terms of (1/v) and p-wave resonance near 250 keV. Some experimental data[1-4] are seemed to be fitted by this characteristic formula. There are, however, several experimental data[5-10] which are seemed to be inconsistent with the above mentioned formula. In the energy region of 10 to 100 keV, the latter data show adifferent trend from (1/v) and are 20-30% higher than those of the former data.

In the present work, preliminary calculations are performed by using the former data. Some cross-section formulae are taken into consideration to fit the experimental data. An interference effect, for example, is investigated between a resonance in the negative energy region and the resonance near 250 keV.

References:

1) M. G. Sowerby et al., AERE-R 6316 (1970).

2) E. Fort, "Nuclear Data for Reactors" (Helsinki Conf.) Vol. I,253 (1970).

3) S. Schwarz et al., Nucl. Phys. 63 (1965) 593.

4) H. Conde et al., FOA 4 Report A4350-411 (1964).

5) J. F. Barry, "Neutron Cross Section Technology" (Washington Conf.) 763 (1966)

---

* CCDN

6) S. A. Cox, "Neutron Cross Section Technology" (Washington Conf.)

7) S. J. Bame et al., Phys. Rev. 114 (1959) 1580.

8) F. Gabbard et al., Phys. Rev. 114 (1959) 201.

9) Gorlov et al., Soviet Phys. Doklady 1, (1956) 705.

10) J. M. Blair et al., ANL-4515 (1950).

I-D-2. Program ELIESE-3; Program for Calculation of the Nuclear Cross Sections by Using Local and Non-Local Optical Models and Statistical Model.

S. Igarasi

Program ELIESE-3 is made for the purpose of calculations for elastic and inelastic scattering cross sections, reaction cross sections and polarizations for particles with spin 0, 1/2 and 1, by the use of spherical local and non-local optical potentials.

By the use of the Program ELIESE-3, following calculations are possible in addition to what are treated by ELIESE-2.

(1) Calculations of the elastic and inelastic scattering cross sections of particles with spin 1.

(2) Calculations of the reaction cross sections concerned with absorptions and emissions of particles with spin 0, 1/2 and 1; for example, (n,p), (d,p), (n, α), etc. These calculations are made by using the Hauser-Freshbach theory and Moldauer theory. Continuous nuclear state is taken into account as well as discrete nuclear levels in the calculations.

(3) Search for the potential parameters in the elastic scattering calculations; fifteen parameters at maximum can be searched for simultaneously.

(4) Calculations of the polarizations, rotations, asymmetries, depolarizations and tensor polarizations of the scattered particles.

(5) Plotting of the angular distributions of the cross sections, polarizations, etc. by using the CALCOMP-plotter.

I-D-3. A Qualitative Study of the Fast Fission Product Cross Sections

M. Kawai*, S. Iijima*, T. Yoshida* and T. Murata*

The systematics of FFP cross sections is being investigated as a part of the JNDC evaluation works of fast fission product cross sections. Firstly, the total cross sections were analyzed by optical potential model. The potential parameters of Engelbrecht-Fiedeldey[1)] were found to give a good fit to the experimental values for nuclides in FP region except near neutron closed shells where the discrepancy amounts to 10-30% for energies below 4 MeV. Reducing the depth of surface absorption potential (derivative Wood-Saxon type) by a factor of two, the better agreement was obtained for these nuclides. The result is shown in Fig. 1. Further check with elastic scattering angular distribution is now in progress. Secondary, the total inelastic scattering cross sections were calculated by a simplified model in comparison with the Hauser-Feshbach theory. This model assumes that the total inelastic scattering cross section is simply proportional to the number of available levels in residual nucleus. By using the constant temperature formula for level density, the total inelastic scattering cross section is written as

$$\sigma_{in}(E) = \sigma_r(E) \frac{T_\rho(E_c)\cdot(\exp(\Delta E/T) - 1)}{1 + T_\rho(E_c)\cdot \exp(\Delta E/T) - 1)}$$

* Nippon Atomic Industry Group Co., Ltd.

where σ_r is the reaction cross section, $\rho(E)$ is the level density, T is the nuclear temperature in the constant temperature level density formula[2], E_c is the effective threshold energy for inelastic scattering, and ΔE is $E - E_c$. This model was shown to give reasonable agreement with Hauser-Feshbach theory results for the typical 10 F.P. nuclides investigated except for La-139 and Pr-141. Therefore, the model will be of use to predict the total inelastic scattering cross sections for nuclides whose level schemes are little understood. Typical results are shown in Fig. 2.

References:

1) C. A. Engelbrecht and H. Fiedeldey: Ann. of Phys. 42 (1967) 262.

2) A. Gilbert and A. G. W. Cameron: Can. J. Phys. 43 (1965) 1446.

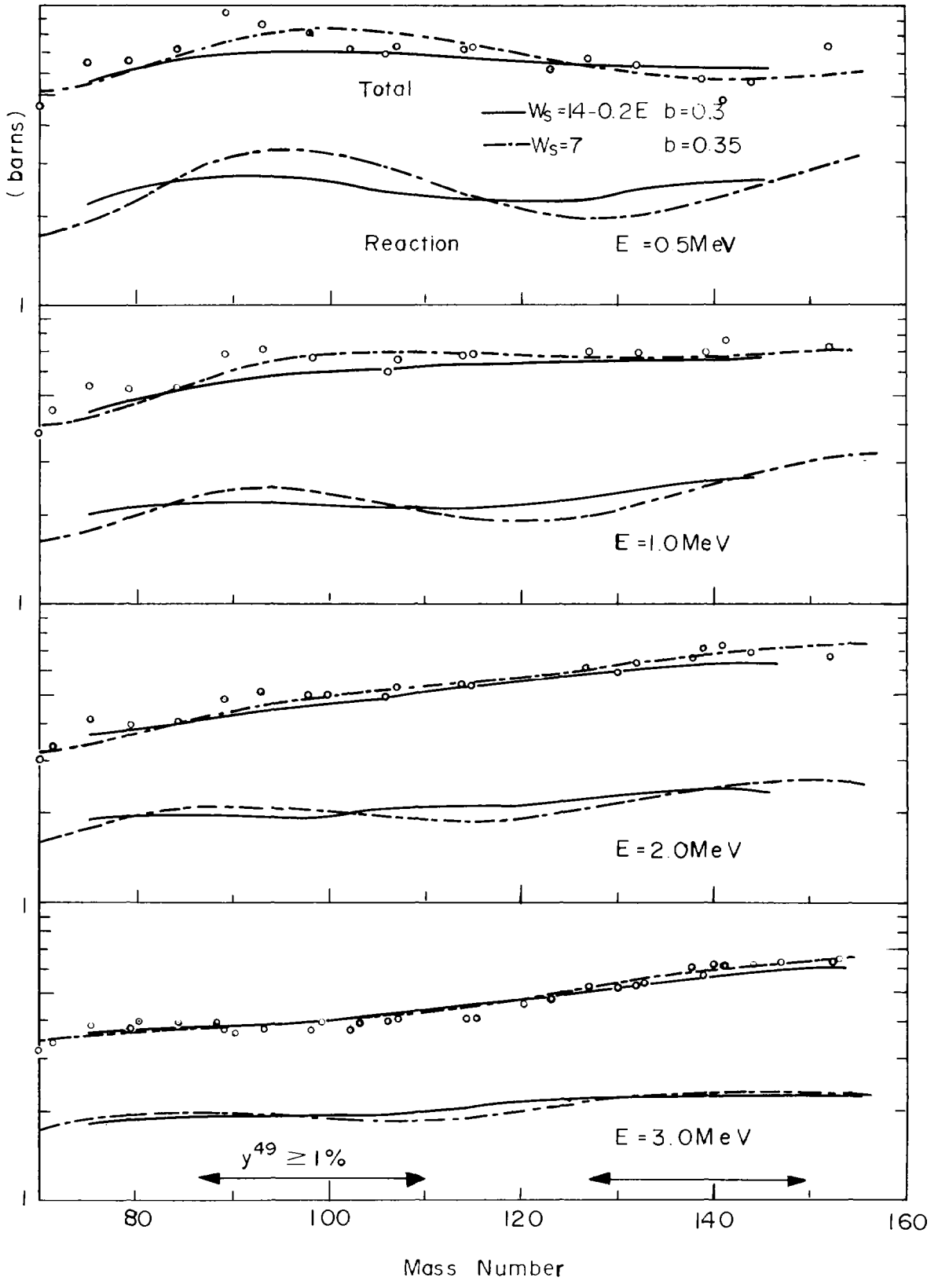

Fig. 1. Optical model calculation of σ_T and σ_R.

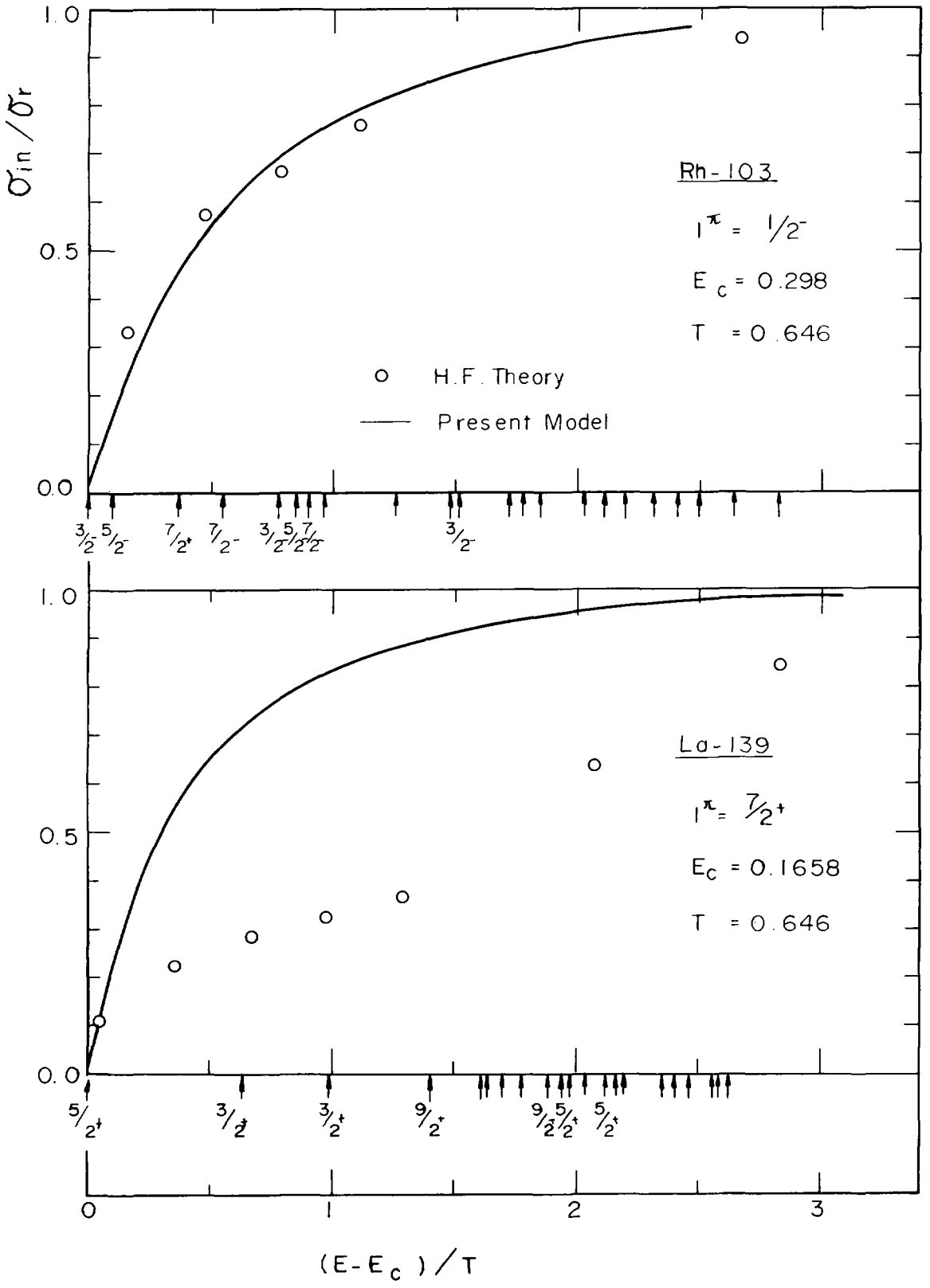

Fig. 2. σ_{in}/σ_r energy dependence for Rh-103, La-139.

II. Kyoto University

A. Research Reactor Institute

II-A-1. Measurements of Total Thermal Neutron Cross Section of Lead, Beryllium and Beryllia

K. Kanda, O. Aizawa*, H. Kadotani**, H. Kawamoto***
and T. Kobayashi

Total cross sections of lead, beryllium and beryllia were measured using a neutron chopper with the heavy water thermal neutron facility of Kyoto University Reactor (KUR), which yeilds a pure Maxwellian neutrons.

Elastic coherent cross sections were calculated with the UNCLE-TOM code.

The measured values agree well with the calculated values. However, they do not agree with the earlier experimental values except beryllium. The example of the present data is shown in Fig. 1.

---

* Research Laboratory of Nuclear Reactor, Tokyo Institute of Technology.

** Century Research Center Co.

*** Hitachi Works, Hitachi Ltd.

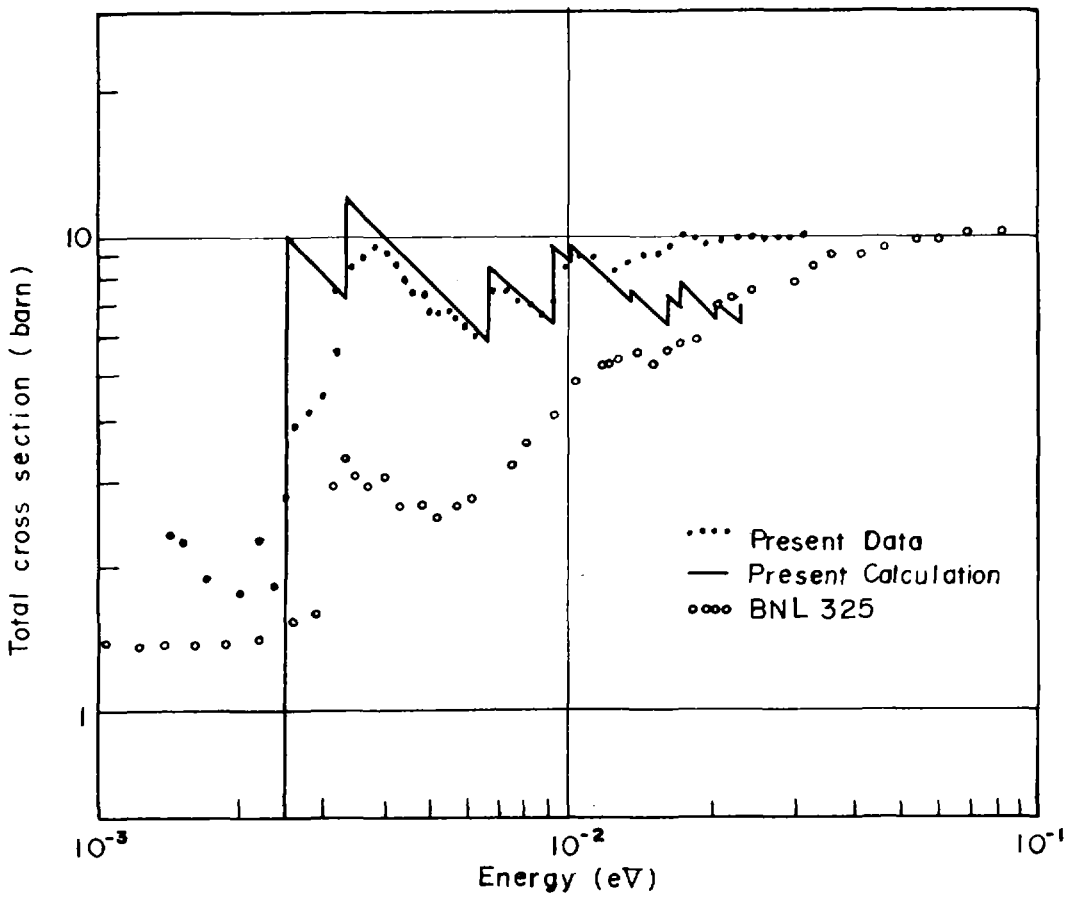

Fig. 1. Measured and calculated cross section of lead at room temperature.

II-A-2. Measurement of Cross Section for $^{115}In(n,n')^{115m}In$ Reaction with a Semiconductor Recoil Proton Counter

Katsuhei Kobayashi, Itsuro Kimura, Hiroshi Gotoh*
and Hideyuki Yagi*

The energy dependent cross section for the $^{115}In(n,n')^{115m}In$ reaction was measured in the energy region from 3.4 MeV to 4.9 MeV. Monochromatic neutrons were produced by $D(d,n)^3He$ reaction with a 2 MeV Van de Graaff accelerator at JAERI. The energy of neutrons was determined by the calculation based on the Fowler & Brolley method[1].

Aiming at improvement of the accuracy of the absolute neutron flux detection, a pair of semiconductor proton recoil counters composed of a polyethylene radiator and a silicon detector was used. One is a main neutron detector just behind the irradiation sample. The other is a neutron flux monitor. The schematic figure of this system is shown in Fig. 1. The details of the detection system are mensioned in elsewhere[2)~4)].

Induced activities of ^{115m}In were measured with a NaI(Tl) scintillation counter whose photopeak efficiency had been calibrated with the standard gamma-ray sources manufactured at IAEA.

Figure 2 shows the present preliminary results of the cross section for the $^{115}In(n,n')^{115m}In$ reaction. The total error of the present result is estimated to be within about 4%.

Finally, the authors calculated the value of the average cross section for the $^{115}In(n,n')^{115m}In$ reaction, making use of the Maxwellian fission neutron spectrum and the energy dependent cross section of the present data and Butler & Santry's data[6] in the energy region except 3.4 MeV to 4.9 MeV. The calculated value becomes to be 176 mb, which agrees well with

* Japan Atomic Energy Research Institute.

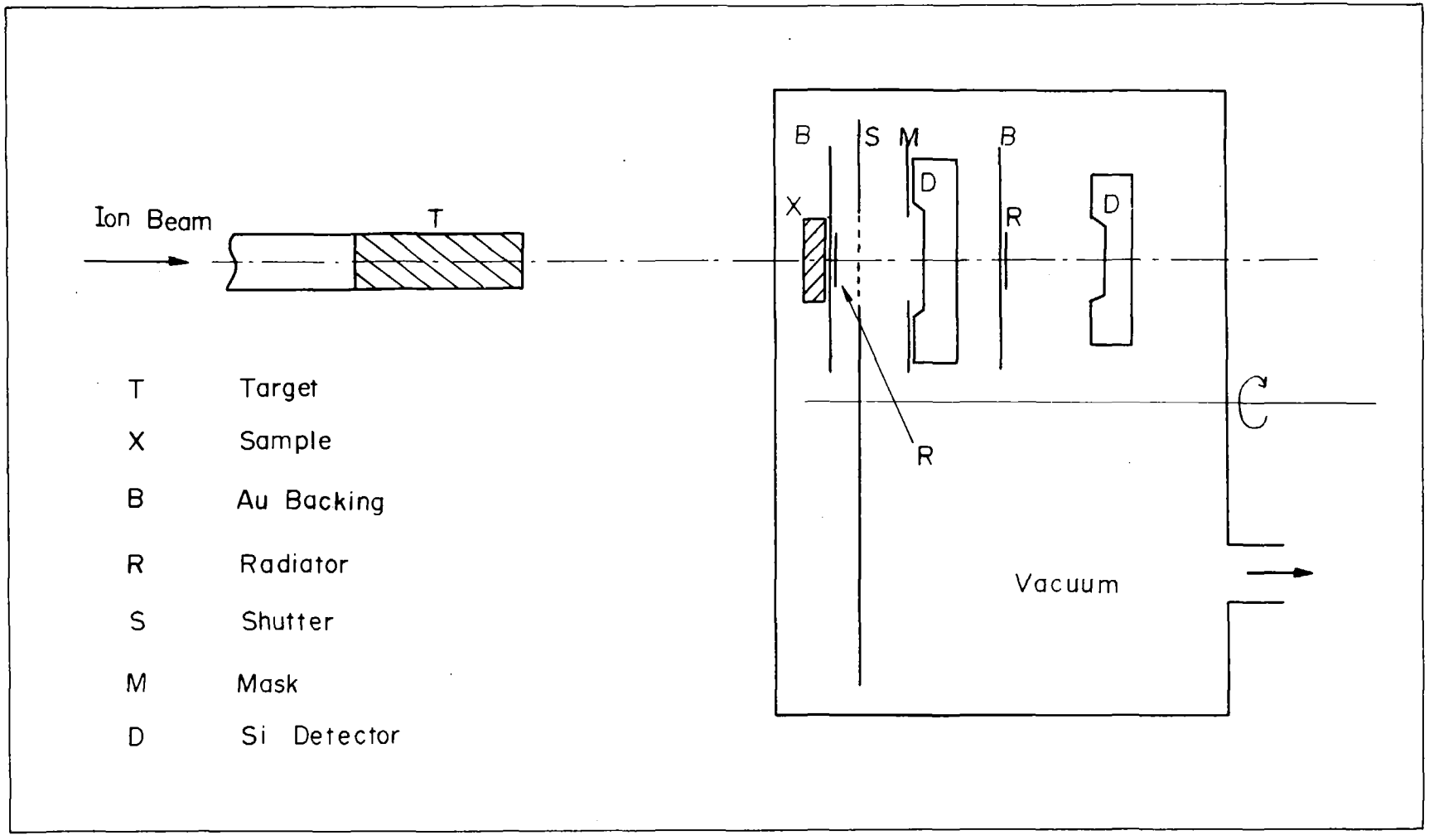

Fig. 1. Schematic figure of a semiconductor recoil proton counter.

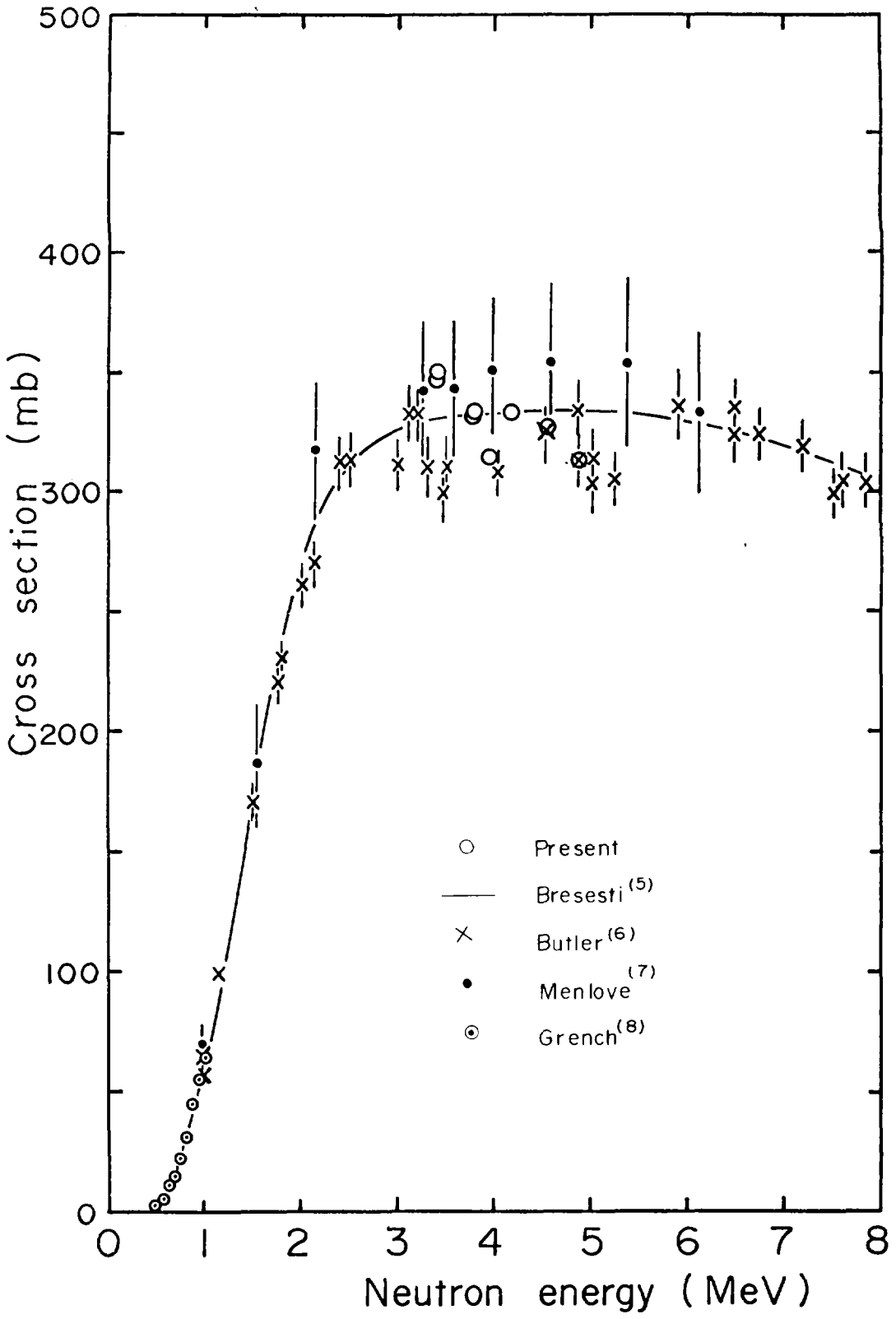

Fig. 2. Cross section for $^{115}In(n,n')^{115m}In$ reaction.

the experimental value 175 ± 2 mb obtained with a fission plate[9].

References

1) J. L. Fowler and J. E. Brolley, Rev. Mod. Phys., 28, 103 (1956).

2) H. Gotoh and H. Yagi, Nucl. Instr. Meth., 97, 419 (1971).

3) H. Gotoh and H. Yagi, ibid, 101, 395 (1972).

4) H. Gotoh, H. Yagi and K. Kobayashi, ibid, 100, 473 (1972).

5) A. B. Bresesti, et al., Nucl. Sci. Eng., 40, 331 (1970).

6) J. P. Butler and D. C. Santry, Bull. Am. Phys. Soc., Series 11, 12, 547 (1967).

7) H. O. Menlove, et al., Phys. Rev., 163, 1308 (1967).

8) H. A. Grench and H. O. Menlove, WASH-1074 (1967).

9) I. Kimura, K. Kobayashi and T. Shibata, IAEA Specialist Meeting on the Status of Prompt Fission Neutron Spectra, Aug. 1971.

II-A-3. Measurements of Cross Sections for ^{237}Np(n,f) and ^{232}Th(n,f) Reactions with a Silicon Detector

Katsuhei Kobayashi and Itsuro Kimura

A chamber composed of a silicon detector and a thin electrodeposited film (about 100 μg/cm^2) of thorium or neptunium was made to measure the cross sections for the ^{237}Np(n,f) and ^{232}Th(n,f) reactions. This direct measurement of fission fragments has an advantage that fission yield data are not necessary. The number of atoms in a sample was determined by alpha-counting. During experiments, neutron flux was monitored with the ^{115}In (n,n')^{115m}In reaction, whose cross sections were separately measured with a semiconductor proton recoil counter[1].

In the present experiments, the cross section, σ is obtained from the following relations;

$$\sigma = \frac{\text{counting rate of fission fragments}}{2\,\epsilon\,N\,\phi}$$

$$= \frac{\lambda \times \text{counting rate of fission fragments}}{2\,\phi \times \text{counting rate of alpha ray}}$$

ϵ : detection efficiency,

N : number of atoms in a sample,

ϕ : neutron flux,

λ : decay constant.

1) Measurement with a Van de Graaff

Though the $^{237}Np(n,f)$ reaction is one of the useful reactions to measure fast neutrons, remarkable discrepancies in its previous cross section values exist in the energy region from about 2 MeV to about 6 MeV. Therefore, the values of the cross section were obtained around 4.5 MeV neutron energy with a 2 MeV Van de Graaff accelerator at JAERI.

Experimental arrangement is shown in Fig. 1. The present preliminary results are depicted in Fig. 2 comparing other works. The error bars are taken account for statistical errors of fission fragments and for the value of neutron monitor due to the $^{115}In(n,n')^{115m}In$ reaction.

Present results are close to the ENDF/B-II data[2].

2) Measurement with the reactor, KUR

The fast neutron spectrum of an experimental beam port E-3 of the Kyoto University Reactor, KUR is close to that of fission neutrons above about 1 MeV[3]. Making use of neutrons with this fission-type reactor spectrum, the average cross sections for the $^{237}Np(n,f)$ and $^{232}Th(n,f)$ reactions were measured with a silicon detector. In this case, the silicon

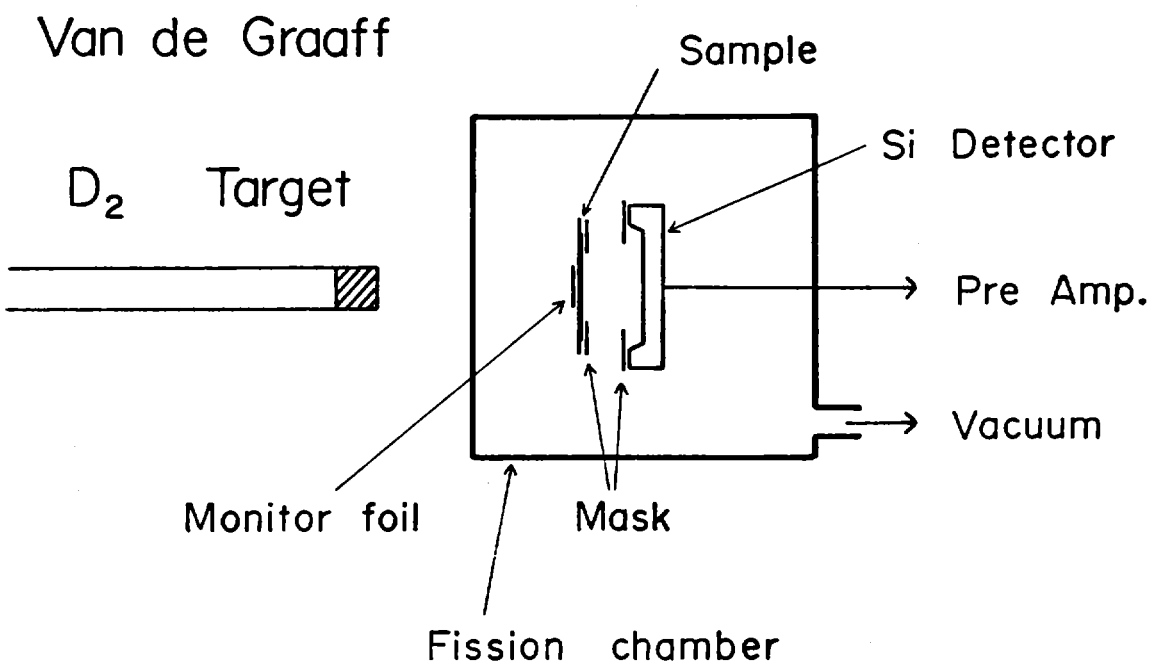

Fig. 1. Experimental arrangement of Van de Graaff.

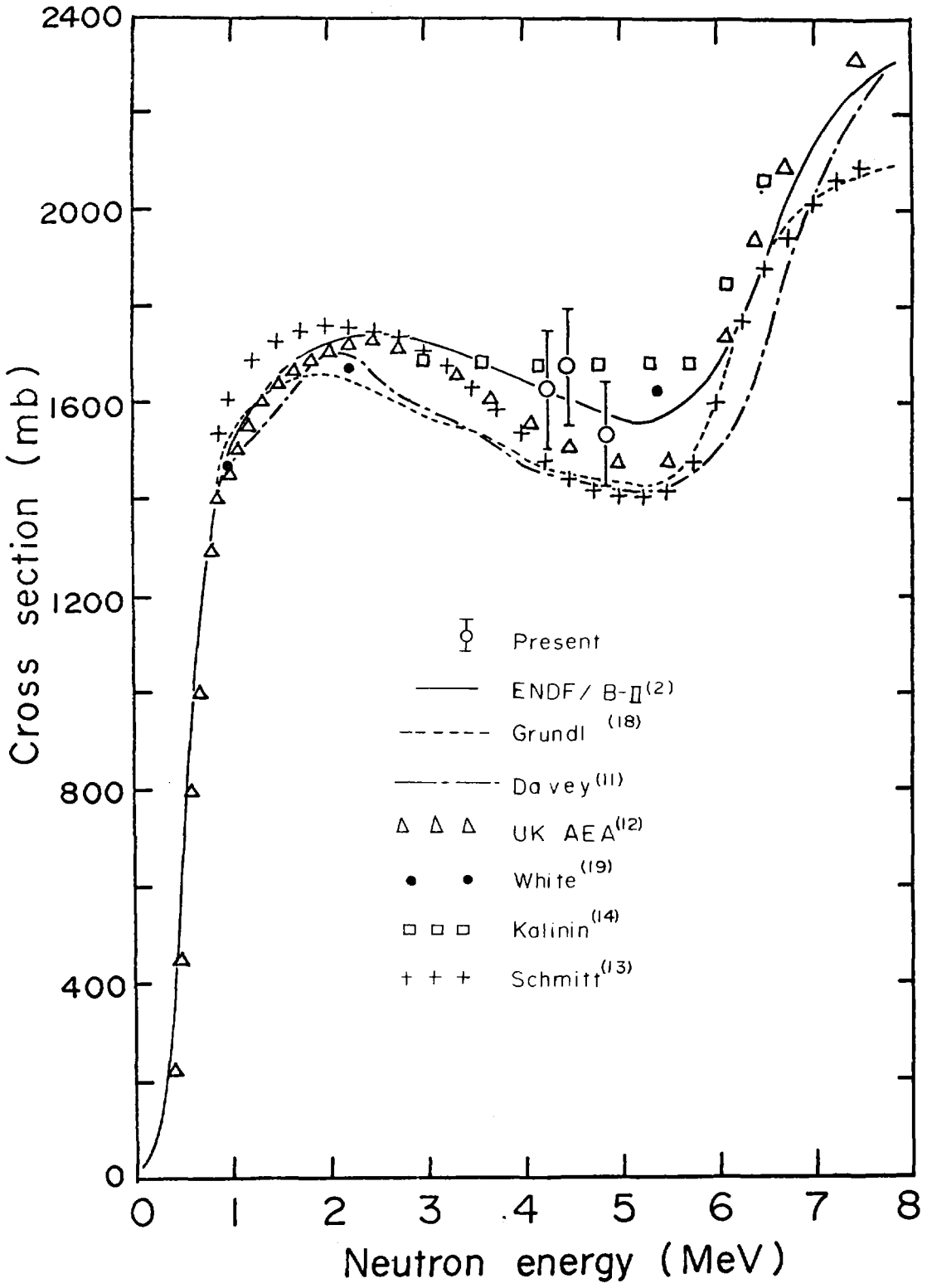

Fig. 2. Cross section for $^{237}Np(n,f)$ reaction.

detector was shielded with lead collimators to avoid intense gamma radiation. Neutrons enter in parallel with the electrodeposited plate.

The present preliminary results of the average cross sections for the ^{237}Np(n,f) and ^{232}Th(n,f) reactions agree with the previous values within the range of experimental errors by the authors, which were obtained by measuring ^{140}La-^{140}Ba activities in irradiated samples and are tabulated in Table 1 and Table 2 comparing other data.

The authors calculated the values of the average cross sections for the ^{237}Np(n,f) and ^{232}Th(n,f) reactions, making use of typical energy dependent cross sections and of two types of fission spectrum (one is previous Maxwellian-type spectrum[9)] and the other is recent SAND-II-type spectrum[10)]). These results are also shown in Table 1 and Table 2.

References

1) K. Kobayashi, I. Kimura, H. Gotoh and H. Yagi, "Measurement of Cross Section for ^{115}In(n,n')^{115m}In Reaction with a Semiconductor Recoil Proton Counter", EANDC in this report.

2) M. K. Drake, BNL-50274 (T-601) 1970.

3) I. Kimura, K. Kobayashi and T. Shibata, J. Nucl. Sci. Technol., 8, 59 (1971).

4) I. Kimura, K. Kobayashi and T. Shibata, IAEA Specialist Meeting on the Status of Prompt Fission Neutron Spectra, Aug. 1971.

5) W. L. Zijp, RCN-Int-63-085 (1963).

6) A. Fabry, Conf. on Radiation Measurements in Nuclear Power, at Berkeley (1966).

7) J. A. Grundl, Nucl. Sci. Eng., 31, 191 (1968).

8) R. L. Simons and W. N. McElroy, BNWL-1312 (1970).

9) L. Cranberg, et al., Phys. Rev., 103, 662 (1956).

10) W. N. McElroy, Nucl. Sci. Eng., 36, 109 (1969).

11) W. G. Davey, ibid, 32, 35 (1968).

12) UKAEA Nuclear Data Library, April 1970.

13) H. W. Schmitt and R. B. Murray, Phys. Rev., 116, 1575 (1959).

14) S. P. Kalinin and V. M. Pankratov, Proc. International Conf. on Peaceful Uses of Atomic Energy, Geneva, Vol. 16, p/2149, p.136.

15) K. Kobayashi and I. Kimura, Ann. Repts., KURRI, 3, 84 (1970).

16) M. Bresesti, et al., Proc. of a Symp., Harwell, 1962, "Neutron Dosimetry", Vol. I, p.27 (1963).

17) B. E. Watt, Phys. Rev., 87, 1037 (1952).

18) J. A. Grundl, Nucl. Sci. Eng., 30, 39 (1967).

19) P. H. White and G. P. Warner, J. Nucl. Energy, Vol. 21, 671 (1967).

Table 1 Comparison of fission average cross sections for $^{237}Np(n,f)$ reaction

Average cross section (barn)	Reference
1.32 ± 0.07	Present work, measured at a beam
1.33 ± 0.11	Our work, measured with a fission plate (4)*
1.323	Zijp's work (5)
1.460	Fabry's work (6)
1.367	Grundl's work (7)
1.293	Simons' work (8)
1.32	ENDF/B(2) + Maxwellian spectrum(9)
1.46	ENDF/B(2) + SAND-II spectrum(10)
1.27	Davey(11) + Maxwellian spectrum(9)
1.40	Davey(11) + SAND-II spectrum(10)
1.31	UKNDL(12) + Maxwellian spectrum(9)
1.16	UKNDL(12) + SAND-II spectrum(10)
1.35	Schmitt(13) + Maxwellian spectrum(9)
1.48	Schmitt(13) + SAND-II spectrum(10)
1.32	Kalinin(14) + Maxwellian spectrum(9)
1.46	Kalinin(14) + SAND-II spectrum(10)
1.31	Grundl(18) + Maxwellian spectrum(9)
1.43	Grundl(18) + SAND-II spectrum(10)

* Measured by counting ^{140}La-^{140}Ba activities.

Table 2 Comparison of fission average cross sections for $^{232}Th(n,f)$ reaction

Average cross section (barn)	Reference
70 ± 6	Present work, measured at a beam port of KUR
67 ± 6	Our work, measured in the core of KUR (15)*
71.9	Bresesti (16)
69	Fabry (6)
72.0	ENDF/B(2) + Watt spectrum(17)
71.4	ENDF/B(2) + Cranberg spectrum(9)
69.0	ENDF/B(2) + Maxwellian spectrum(9)
85.3	ENDF/B(2) + SAND-II spectrum(10)
76.4	UKNDL(12) + Watt spectrum(17)
75.6	UKNDL(12) + Cranberg spectrum(9)
73.2	UKNDL(12) + Maxwellian spectrum(9)
90.8	UKNDL(12) + SAND-II spectrum(10)

* Measured by counting ^{140}La-^{140}Ba activities.

II-A-4. Direct Measurement of Gamma-Ray Energies and Half-Life of ^{141}Cs Separated by Paper Electrophoresis

T. Tamai, J. Takada, R. Matsushita and Y. Kiso

A paper on this subject was published in J. Nucl. Sci. Technol. 9, 378 (1972).

The Cs and Rb from fission products were separated at migration time of 10 s by paper electrophoresis. The gamma-rays from Cs and Rb nuclides were measured by a Ge(Li) detector of 30 cm^3 active volume. The gamma-ray energies and the intensity were determined using an OKITAC-5090H computer. The main photopeaks observed were attributed to ^{90}Rb, ^{91}Rb, ^{140}Cs and ^{141}Cs. The energy and relative intensity of gamma-rays emitted from ^{141}Cs are given in Table 1. The half-life of ^{141}Cs obtained was 25 s.

Table 1 The energy and relative intensity of the gamma-rays emitted from Cs-141

Published Data*	Present Data	
Energy (KeV)	Energy (KeV)	Relative Intensity (%)
---	439	65 ± 10
540	537	13 ± 10
557	555	61 ± 30
563	562	100
590	589	90 ± 8
---	693	67 ± 16
---	1042	58 ± 31
---	1130	49 ± 6
---	1147	50 ± 12
---	1543	52 ± 13

* G.C. Carlson et al.: Nucl. Phys., A 125, 267 (1969).

B. Institute of Atomic Energy

II-B-1. Mass Yields of ^{241}Am Thermal-Neutron Fission

H. Nakahara*, I. Fujiwara, H. Okamoto**, N. Imanishi,
M. Ishibashi and T. Nishi

A full paper on this subject was published in J. Inorg. Nucl. Chem. 33 (1971) 3239 with an abstract as follows:

Mass yields of sub-threshold fission induced by thermal neutrons were investigated, namely, mass yields of 23 mass chains were determined for ^{241}Am thermal-neutron fission by the conventional radiochemical method and by the direct γ-ray spectrometry method. The peak-to-trough ratio in terms of ^{99}Mo/^{117}Cd was found to be as large as 800±200. Three fission systems of spontaneous fission, sub-threshold fission and above-threshold fission with the compound mass A_F = 242 were compared and discussed. The average number of neutrons released per fission was evaluated to be 4.0 ± 0.2 from the mass yield curve.

Present address: * Faculty of Science, Niigata University.
** Power Reactor and Nuclear Fuel Development Corporation.

III. Kyushu University
Department of Nuclear Engineering

III-1. The Excitation Functions and Isomer Ratios for Neutron-Induced Reactions on ^{92}Mo and ^{90}Zr

Y. Kanda

A full paper of this work, which was outlined in the previous report (EANDC(J)22L p.32), was published in Nuclear Physics A185 (1972) 177-195 with an abstract as follows:

Absolute cross sections of the reactions ^{92}Mo(n,2n)^{91m,91g}Mo, ^{92}Mo(n,p)^{92}Nb and ^{92}Mo(n,α)^{89m,89g}Zr, relative cross sections of the reaction ^{90}Zr(n,2n)^{89m}Zr and isomer ratios of the ^{90}Zr(n,2n) reaction have been measured in the neutron energy range 13-15 MeV. The results for the (n,2n) reactions are in good agreement with those of the previous studies. The present results for the (n,p) and (n,α) reactions are in disagreement with the previous works. The experimental data are analysed by the statistical model to determine the level-density parameter a, the moment of inertia I and the strength of the γ-ray transition S_ℓ in order to simultaneously reproduce the experimental data on the excitation function and the isomer ratio in the (n,2n) reaction. The γ-ray competition, the yrast level and the experimental information on the excited levels of the residual nucleus in the (n,2n) reaction are taken into account. The obtained values of a, I and S_ℓ are consistent with those deduced from other types of nuclear data.

III-2. The Energy Spectra of The Alpha Particles in The Fission of ^{252}Cf

K. Tsuji, A. Katase, T. Katayama, Y. Kanda, H. Yamamoto
and Y. Yoshida

The energy spectra of the alpha particles in the fission of ^{252}Cf were measured at four angles to fission fragments. These spectra were sorted by the kinetic energy of the light or heavy fission fragments. The results are shown in Fig. 1. θ_L is an angle between the alpha particles and the light fragments. The average energy of alpha particles above 11 MeV is shown in Fig. 2 as a function of the angle θ_L. The present result shows the larger variation of the average energy than the result of Fraenkel[1].

Further measurements are now in progress.

Reference:

1) Z. Fraenkel: Phys. Rev. 156 (1967) 1283.

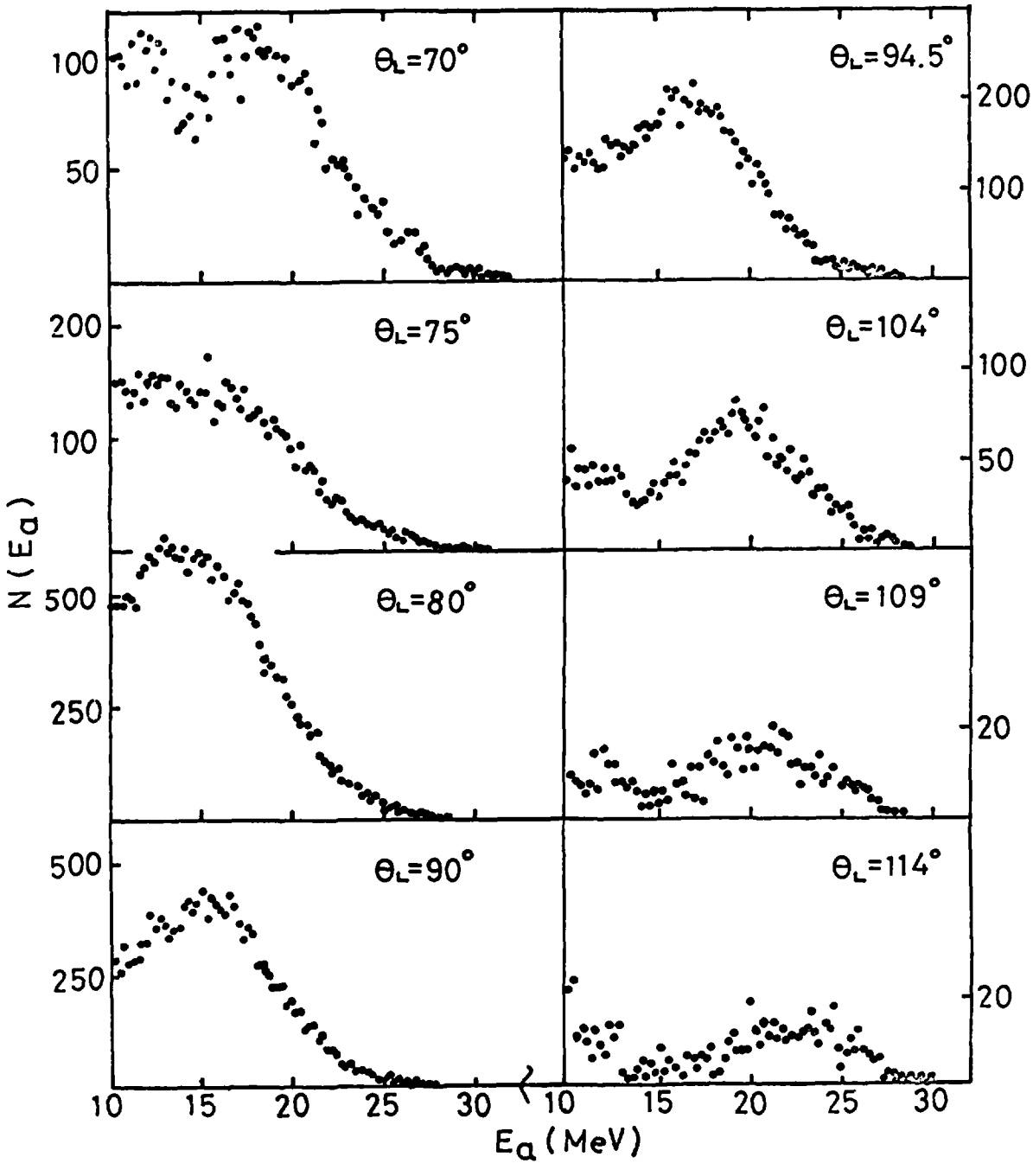
θL=70°
θL=94.5°
θL=75°
θL=104°
θL=80°
θL=109°
θL=90°
θL=114°
N (Eα)
Eα (MeV)
100
50
200
100
200
100
100
50
500
250
20
500
250
20
10
15
20
25
30
10
15
20
25
30

Fig. 1.

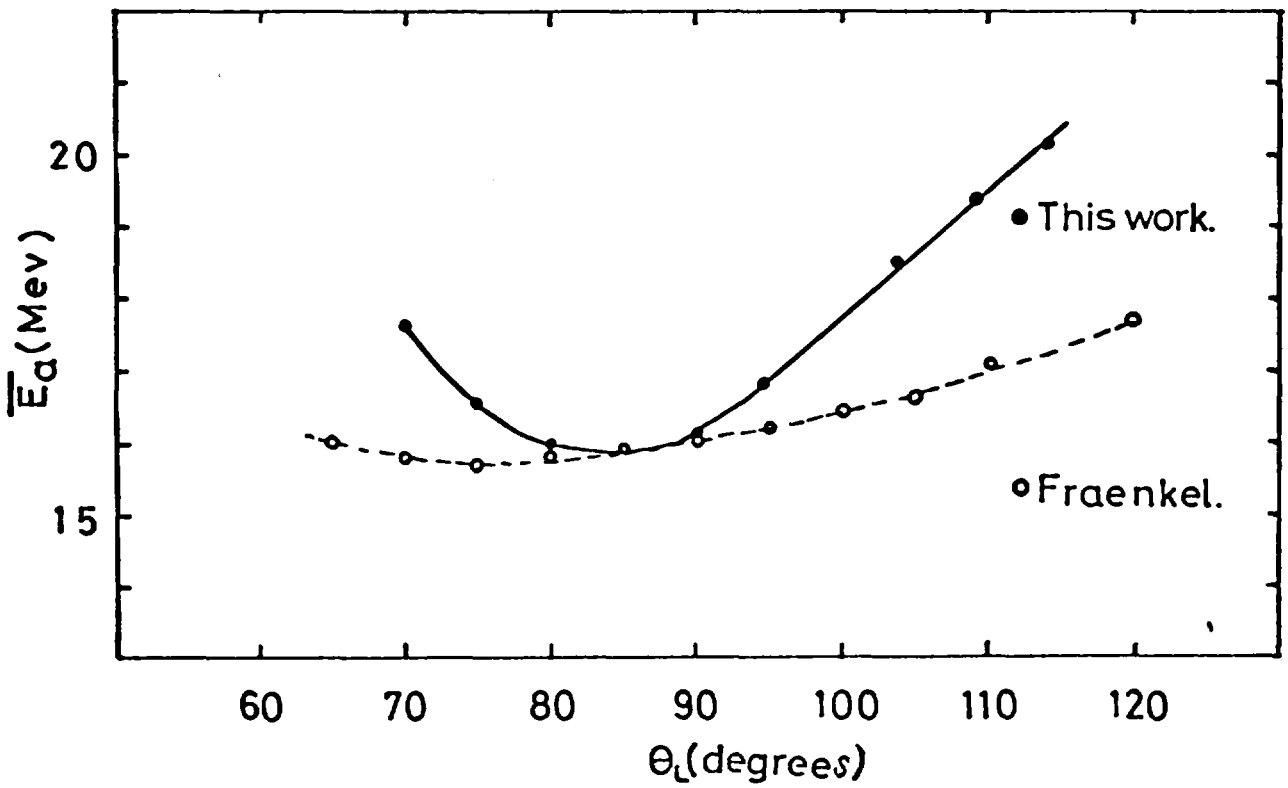
20
15
$\overline{E}_\alpha$(Mev)
60
70
80
90
100
110
120
θ_L(degrees)
• This work.
o Fraenkel.

Fig. 2.

IV. Osaka University

A. Department of Physics

IV-A-1. (N-Z) Dependence of (n, γ) Cross Sections

K. Matsuoka, I. Isomoto, M. Sano, S. Igarasi* and
K. Nishimura*

Experimental data of the (n, γ) reaction cross section have been accumulated for many elements, but few investigations were made about the systematics of the reaction cross section.

We explored regularities of the (n, γ) cross sections in low energy region. Two characteristics were found:

(1) The (n, γ) cross sections above resonance energy region decrease gradually with the increase of the neutron excess (N-Z) of target nucleus.

(2) The systematics (1) is not satisfied for nuclei with the magic neutron numbers and for nuclei in the transitional region from spherical to deformed shape.

We clarify origins of the characteristics mentioned above. One of them is the (N-Z) dependence of the neutron separation energy, and the other is the shell effect for the level density.

The neutron capture probability increases as the separation energy and the number of energy levels increase. The separation energy decreases generally with the increase of (N-Z), except for the region of the closed shell. The number of energy levels of the final states decreases as the potential depth for the incident neutron becomes shallow. These are owing to the symmetry term in the average potential for the incident neutron, by

* Japan Atomic Energy Research Institute.

which the potential depth becomes shallow with the increase of (N-Z). As the result, the neutron capture cross section decreases as the neutron excess (N-Z) increases.

We calculated the (n, γ) cross sections for Te, Nd and Dy isotopes by using the computer code RACY. The detailed calculations for other nuclei are now in progress.

B. Department of Nuclear Engineering

IV-B-1. Intermediate Resonances in the Neutron Total Cross Section of U^{235} at Low Energies

Y. Kitazoe, H. Suzuki and T. Sekiya

A paper on this subject is in press in Atomkern Energie with an abstract as follows:

The formal theory of nuclear reactions derived in a previous paper is applied to investigate the existence of intermediate resonances in the neutron total cross section of U^{235} at low energies (E = 0 ~ 300 ev). A particular attention is paid to clarify a relation between the most complicated mechanism states (compound nucleus states) and simpler mechanism states. The theory is compared with the R-matrix theory from the theoretical point of view and, at the same time, through the practical evaluation of the cross section of U^{235}. The evaluated cross section is in good agreement with experiment from a qualitative view point.

IV-B-2. Calculation of Rotational Frequencies of Organic Moderator Molecules

T. Sekiya and K. Sakamoto*

A paper on this subject is to be published in Tech. Repts. Osaka Univ. with an abstract as follows:

The rotational and lattice-vibrational structure of benzene lattice is analysed by GF matrix method. The numerical results of frequency

---

* Department of Applied Mathematics, Okayama College of Science, Okayama.

distribution show good agreement of peak positions with several neutron scattering data. The essential difference of total neutron cross section data near the melting point between benzene and polyphenyls is explained from the rotational mechanisms of these molecules.

V. Tokyo Institute of Technology
Research Laboratory of Nuclear Reactor

V-1. Neutron Transmission Measurement of Pd

N. Yamamuro, H. Yokobori, O. Aizawa, I. Kimura*,
T. Akiyoshi* and T. Ebisawa*

Neutron transmission measurement of Pd over the energy range from 10 eV to 300 eV has been carried out by the use of the usual LINAC-TOF technique. The experimental resolutions were 50 nsec/m at 300 eV and 100 nsec/m at 10 eV. Sample thicknesses used were 1.6 mm and 5.3 mm, and the neutron detector was a ^{6}Li glass scintillator of 12.7 cm in diameter and 1.27 cm in thickness.

The neutron widths of resonances were extracted from the data by Atta-Harvey area-analysis method. The resonance parameters determined preliminarily are shown in Table 1. The values of the neutron width agreed well with that of the recommended values of BNL-325, except for the 33.1 eV resonance.

* Research Reactor Institute, Kyoto University.

Table 1 Resonance Parameters of Pd

	E_0(eV)	J	Γ(mV)	Γ_n(mV)	
				Present	BNL-325
	11.70±0.05	3	149± 3	0.19±0.01	0.19±0.01
^{105}Pd	13.2 ±0.1	2	172± 3	3.2 ±0.1	2.9 ±0.2
$I^{\pi}=5/2^{-}$	25.1 ±0.1	3	150± 7	3.4 ±0.3	3.0 ±0.3
	55.2 ±0.3	3	158±20	7.1 ±0.9	7.2 ±0.3
	68.4 ±0.5	3		2.1 ±0.4	1.8 ±0.3
	78.0 ±0.5	2		19.2 ±4.0	17 ±3
	87.0 ±0.5	3		16.7 ±2.5	16 ±3
	127 ±2	3		2.5 ±1.5	3.13±0.81
	142 ±2	2		12.9 ±4.6	11.6±2.1
^{108}Pd	33.1±0.2			124 ± 4	80 ± 20
$I^{\pi} = 0^{+}$	91 ±1			203 ±17	150 ± 60

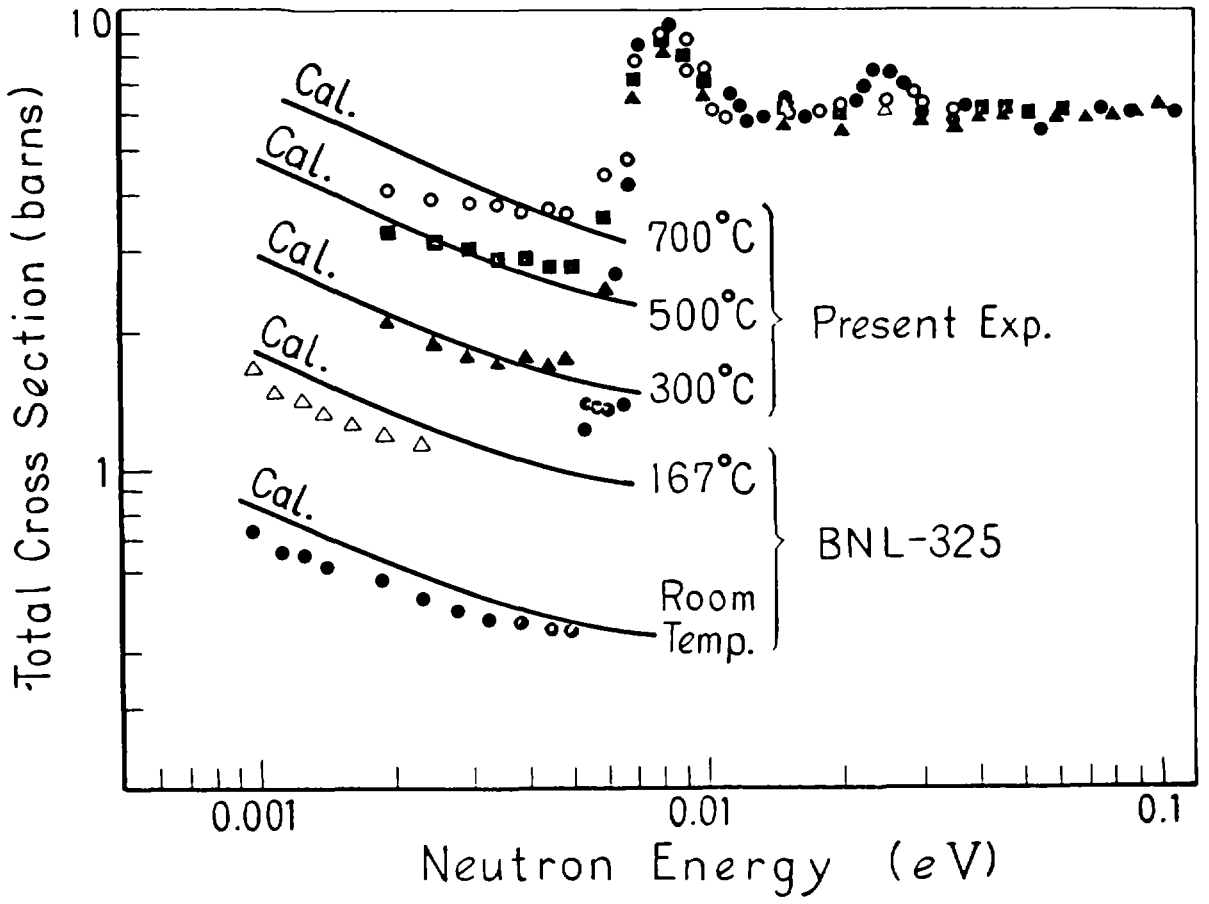

Fig. 1. Total cross section of beryllium.

V-2. Thermal Neutron Scattering Cross Section of Beryllium

O. Aizawa, K. Kanda* and Y. Fukano

The total scattering cross section of beryllium in the energy range of 0.002 to 0.3 eV was measured by transmission technique at four temperatures of scattering sample: 23, 300, 500 and 700°C. The experimental values were in good agreement with the calculated ones, which were performed by the use of the spectral density function evaluated by a working group of the Japanese Nuclear Data Committee[1]. The results are shown in Fig. 1.

References:

1) S. Iijima et al., "Evaluation of Thermal Neutron Scattering Cross Sections for Reactor Moderators" JAERI 1181 (1969).

V-3. Level Structure of ^{54}Mn from the ^{54}Cr(p, nγ) reaction

M. Ogawa and H. Taketani**

Excitation functions and angular distributions of gamma-rays in the ^{54}Cr(p, nγ) reaction were measured in order to establish the spins and parities of the ^{54}Mn levels. Gamma-ray spectra from the ^{51}V(α, nγ) reaction were analysed by using the theoretical predictions of the statistical compound nucleus model[1].

Gamma-ray spectra from the ^{54}Cr(p, nγ) and ^{51}V(α, nγ) reactions are

---

* Research Reactor Institute, Kyoto University.

** Department of Applied Physics, Tokyo Institute of Technology.

shown in figure 1 and figure 2, respectively. The excitation functions of the gamma-rays from the $^{54}Cr(p, n\gamma)$ reaction are shown in figure 3. Gamma-gamma coincidences in the $^{54}Cr(p, n\gamma)$ reaction were also observed using two Ge(Li) detectors. In figure 4, a sample of the $\gamma - \gamma$ coincidences is shown. The result of the γ-ray excitation functions and the $\gamma - \gamma$ coincidences confirmed the existence of a new level at 1391 keV excitation. In the measurement of the γ-ray angular distributions, the incident proton energies were chosen to be 50-400 keV above the thresholds. The angular distributions of the γ-rays obtained are shown in figure 5. In figure 6, the experimental coefficients A_2 and A_4 of the Legendre polynomial expansion are compared with the theoretical A_2-A_4 curves. Considering the result of the γ-ray excitation functions as well as that of the γ-ray angular distributions, unique spin assignments were obtaind for the 54.5 keV (2^+), 156.2 keV (4^+), 368.1 keV (5^+), 407.4 keV (3^+), 1009.9 keV (3^+) and 1374.5 keV (2) levels in ^{54}Mn. The most probable spins were found for the other levels up to 1.5 MeV excitation. With respect to the parities of the levels, the results of the other direct reactions[2,3] are used. A level scheme of ^{54}Mn obtained from the present work is shown in figure 7. Summary of E_2-M_1 mixing ratios of the γ-rays is given in table 1.

References:

1) E. Sheldon and D. M. Van Patter, Rev. Mod. Phys. 38 (1966) 143.

2) S. A. Hjorth, Arkiv Fysik 33 (1966) 147.

3) L. L. Lynn, W. E. Dorenbusch, T. A. Belote and J. Rapaport, Nucl. Phys. A, 135 (1969) 97.

4) P. A. Moldauer, Nucl. Phys. 47 (1963) 65.

5) E. H. Auerbach and F. G. Perey, BNL 765 (1962).

6) F. G. Perey, Phys. Rev. 131 (1963) 745.

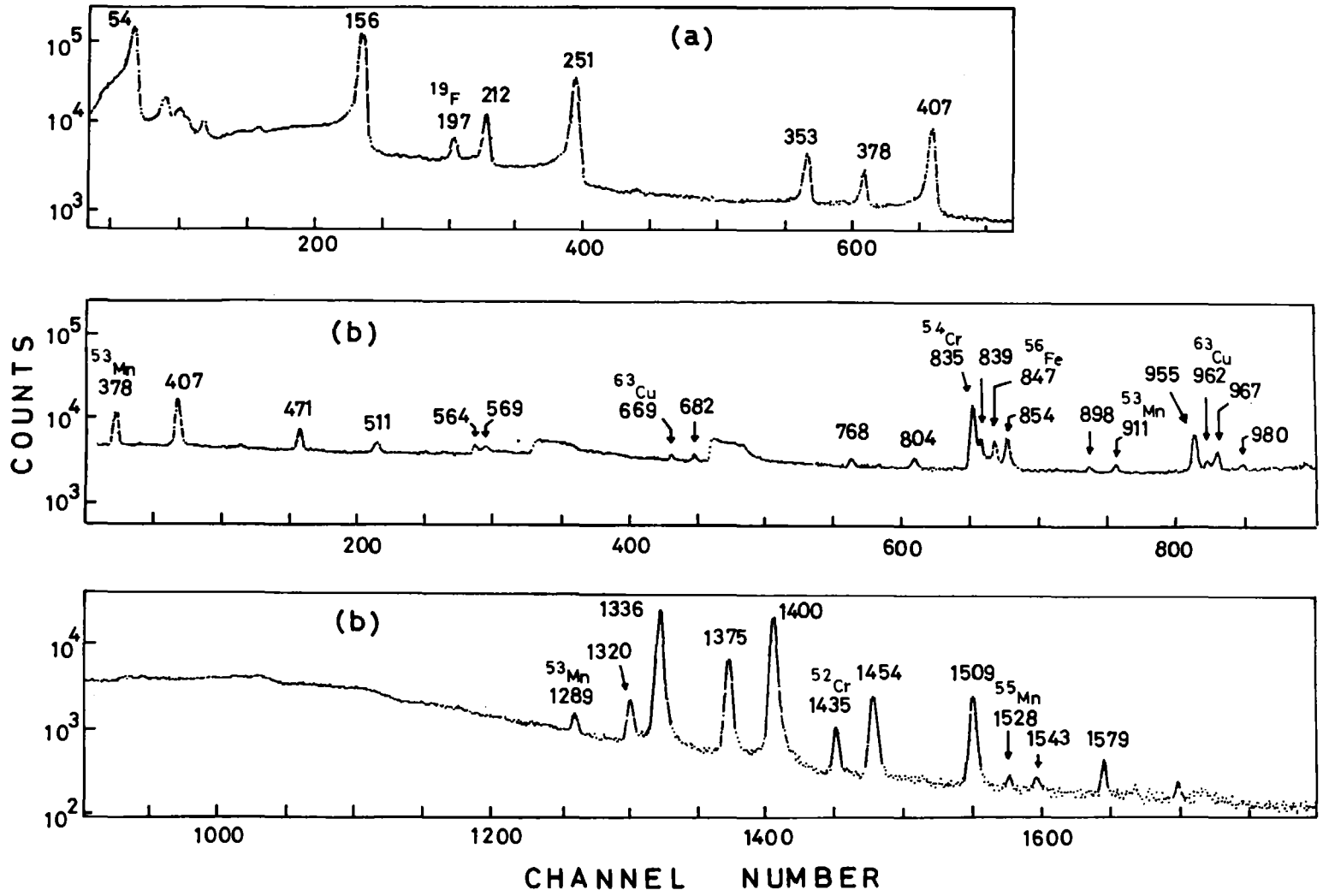

Fig. 1 Singles γ-ray spectra from the $^{54}Cr(p,n\gamma)$ reaction. Low-energy γ-rays of (a) were observed at E_p = 3.65 MeV and high-energy γ-rays of (b) at E_p = 3.90 MeV. Gamma-ray energies are given in keV.

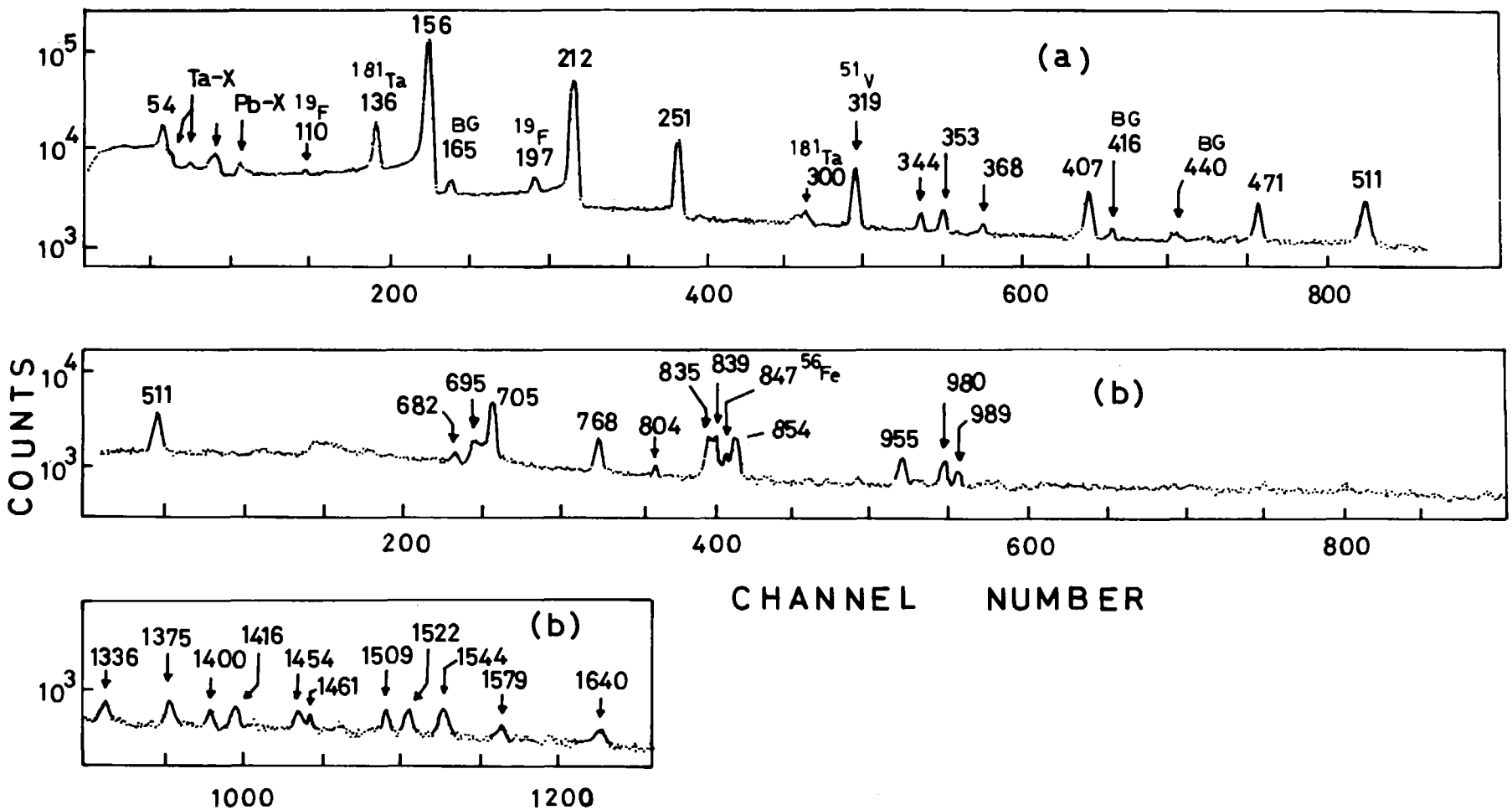

Fig. 2 Singles γ-ray spectra from the $^{51}V(\alpha,n\gamma)$ reaction. These spectra were obtained by summing two different spectra; the one observed at E_α = 7.6 MeV with a integrated beam charge Q of 75 μ Coulomb and the other at E_α = 7.1 MeV with Q = 106 μ Coulomb. Low-energy γ-rays are shown in (a) and high-energy γ-rays in (b). BG means γ-rays observed when the vanadium target is replaced by a gold target.

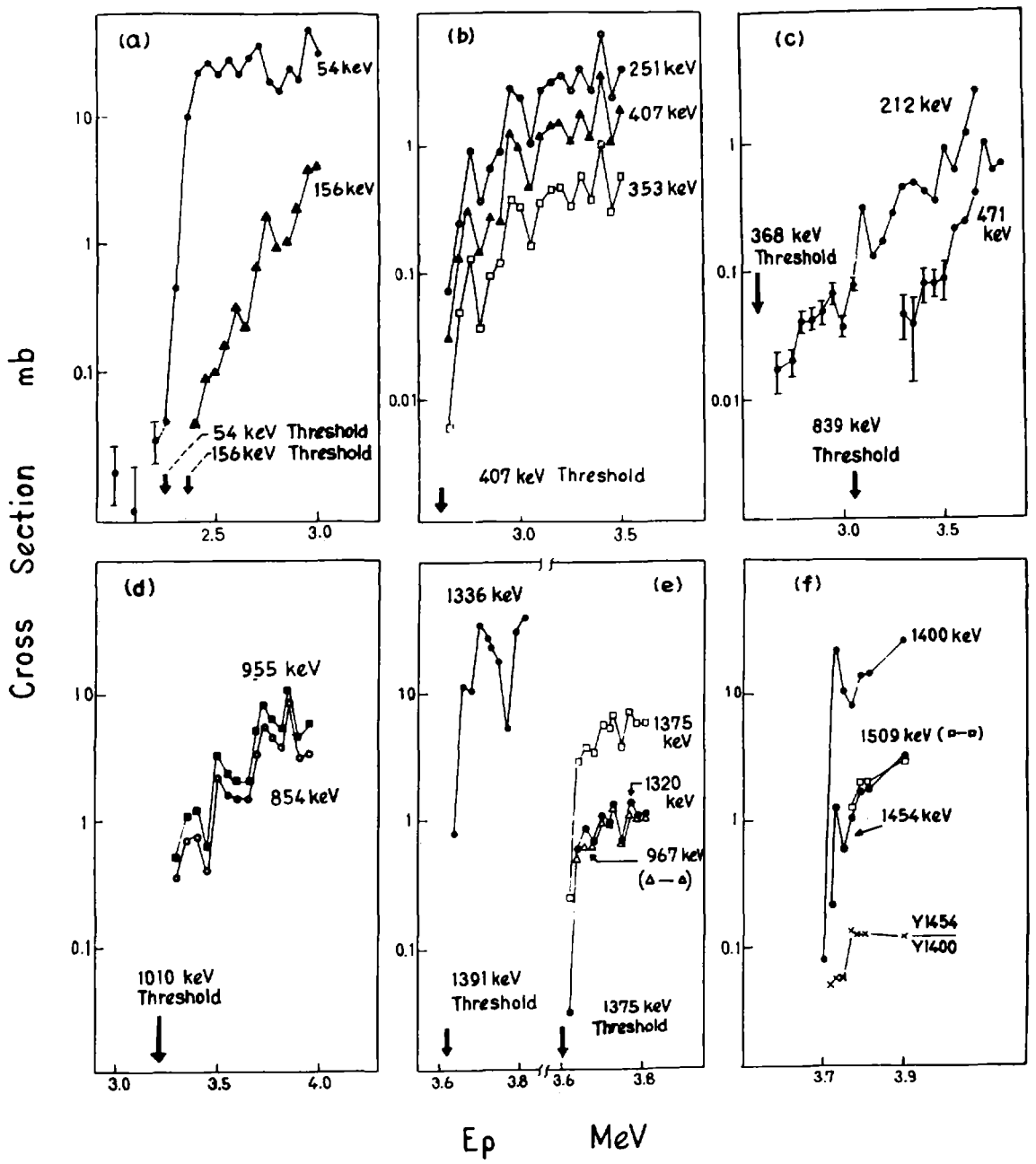

Fig. 3 Excitation functions of γ-rays from the $^{54}Cr(p,n\gamma)$ reaction. In (a), (b), (c) and (d), incident proton energy was varied in steps of 50 keV and in (e) and (f) mostly in steps of 20 keV. Expected thresholds of levels are indicated with arrows. In (f), Y1454/Y1400 indicates the ratio of the 1454 keV γ-ray yield to the 1400 keV γ-ray yield. In this case, the scale of the ratio is same as that for the cross section (mb).

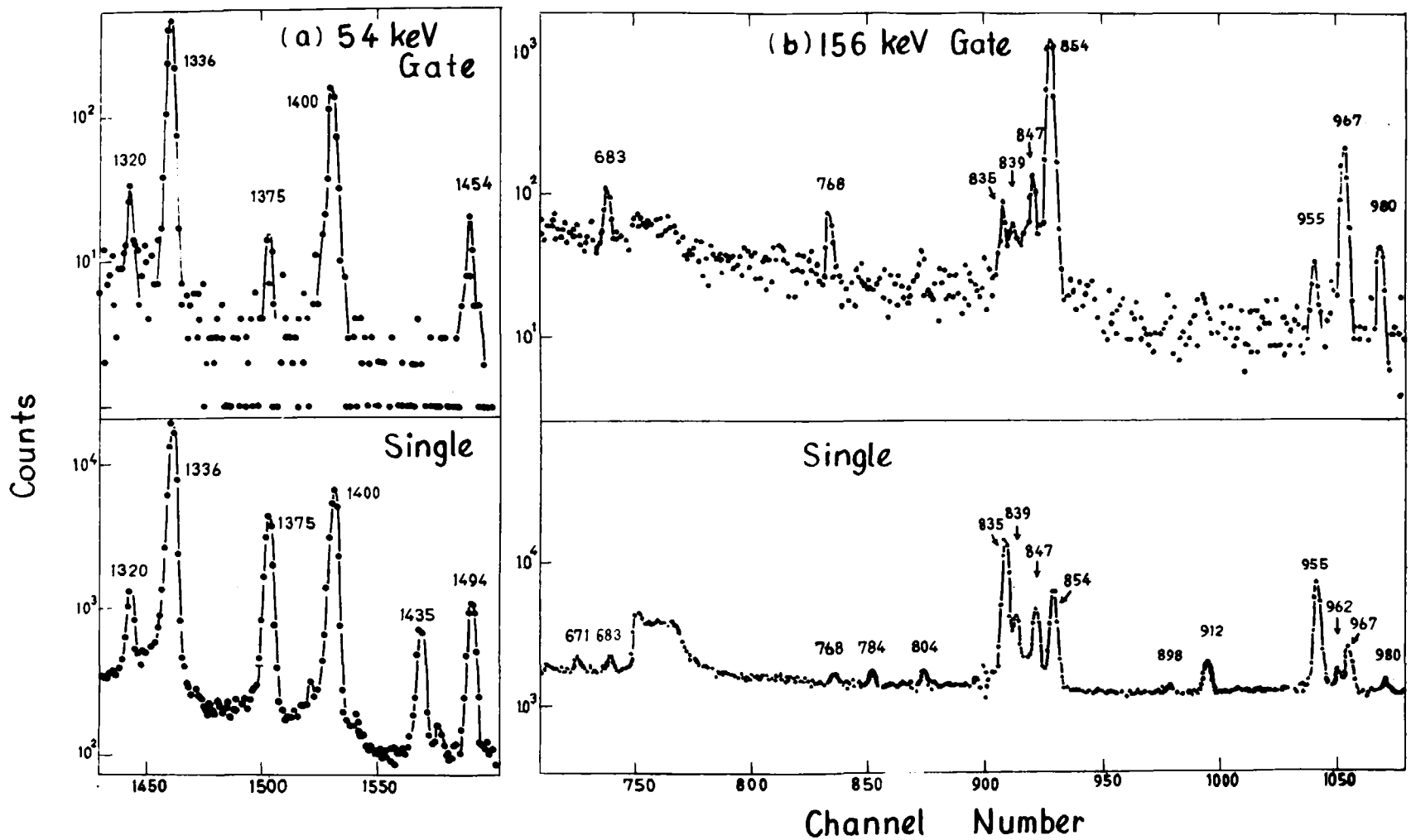

Fig. 4 Gamma-gamma coincidence spectra in the $^{54}Cr(p,n\gamma)$ reaction. These spectra were obtained at E_p = 3.80 MeV using a Ge(Li)-Ge(Li) coincidence system. A sample of γ-ray spectra in coincidence with the 54 and 156 keV γ-rays are shown in the upper-halves of (a) and (b), respectively. No corrections due to accidental coincidences are made for the coincidence spectra. Singles γ-ray spectra are also given in the lower-halves.

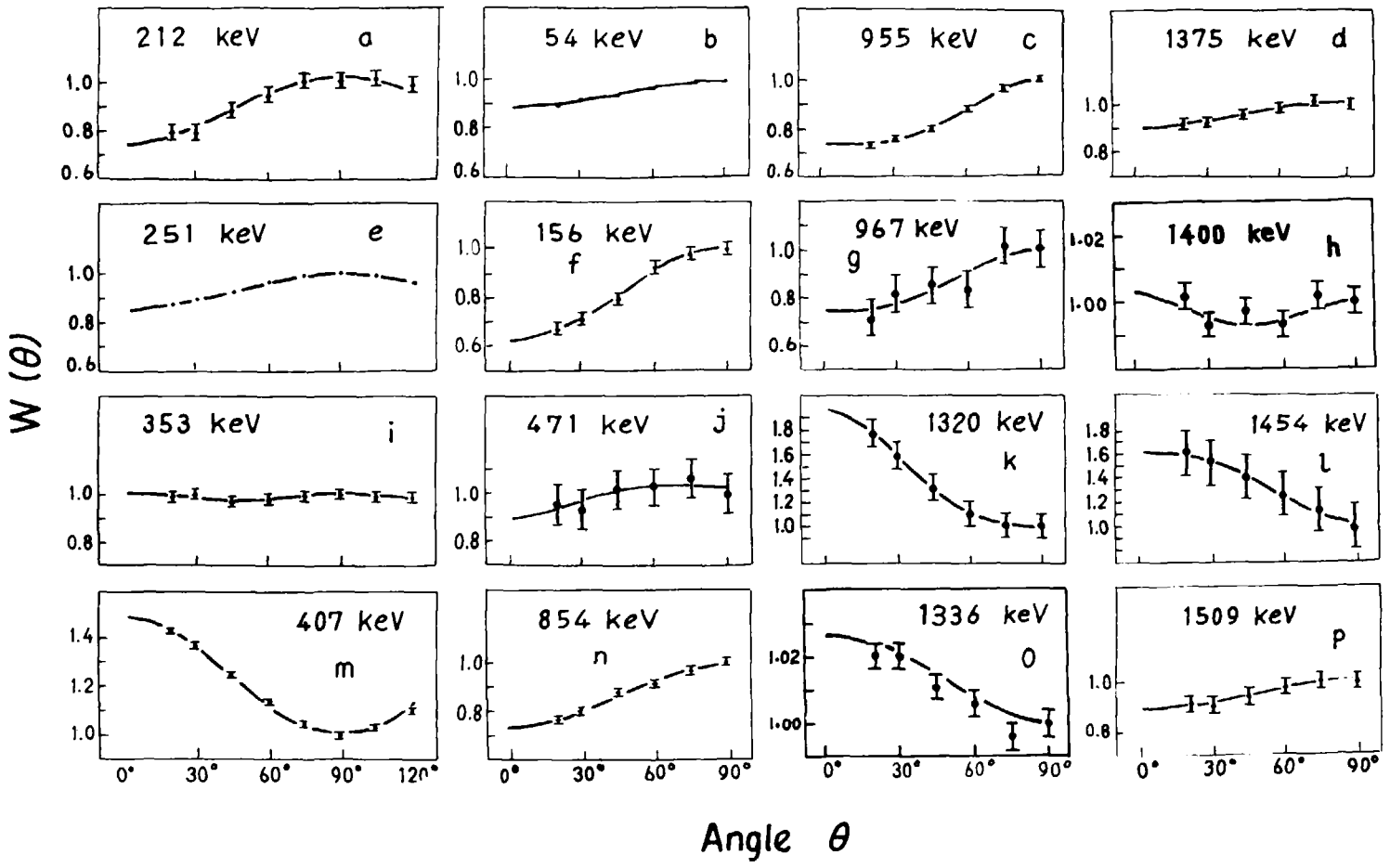

Fig. 5 Gamma-ray angular distributions in the $^{54}Cr(p,n\gamma)$ reaction. The angular distributions of (a), (e), (i) and (m) were measured at eight angular positions and the others at six angular positions. Incident proton energies are E_p = 2.45 - 2.49 MeV in (b), E_p = 2.55 - 2.59 MeV in (f), E_p = 2.94 - 2.98 MeV in (a), (e), (i) and (m), E_p = 3.35 - 3.39 MeV in (c), (j) and (n) and E_p = 3.80 - 3.84 MeV in the others. All the distributions are normalized at θ = 90°. Solid curves indicate least squares fits.

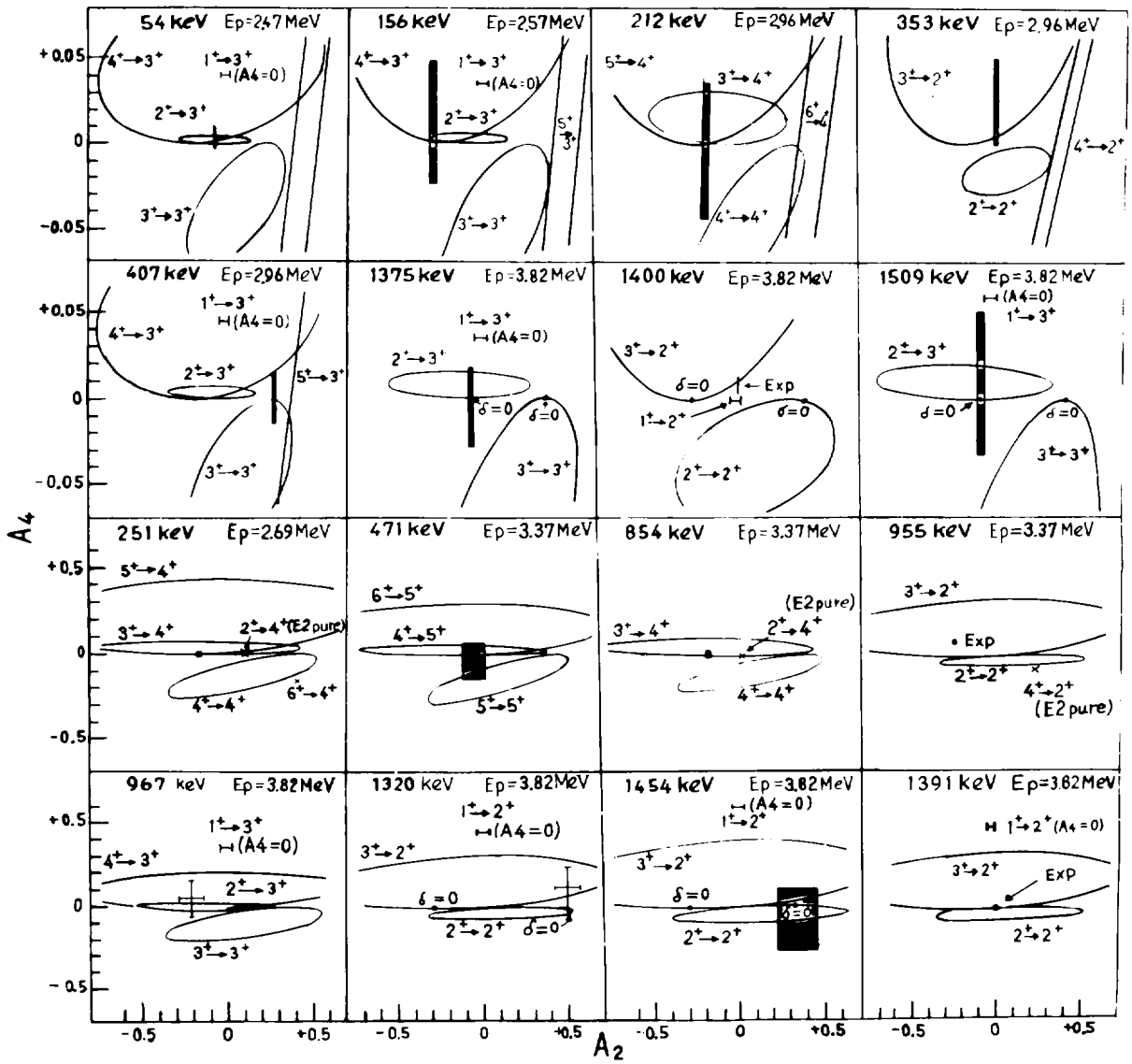

Fig. 6 A comparison of the experimental γ-ray angular distributions with theory in the $^{54}Cr(p,n\gamma)$ reaction. Theoretical Legendre coefficients shown were obtained from the theoretical expressions of Sheldon and Van Patter[1]. The transmission coefficients used are those from a Perey set of V = 52 MeV and W = 11.5 MeV for protons and those from the average parameters of Moldaer for neutrons. The multipole mixing ratio was varied as a parameter. Theoretical curves of A_2-A_4 for the spin sequences, which are not probable from the other considerations, are not indicated. In the case of 1^+-- 2^+ or 1^+-- 3^+ sequence, the coefficient A_4 is always 0 and the possible region of A_2 is indicated. In the case of 2^+ – 4^+, 4^+ – 2^+ or 6^+ – 4^+ sequence, a point corresponding to a pure E2 transition is indicated with a cross. The incident proton energy shown is the middle one of the chosen values.

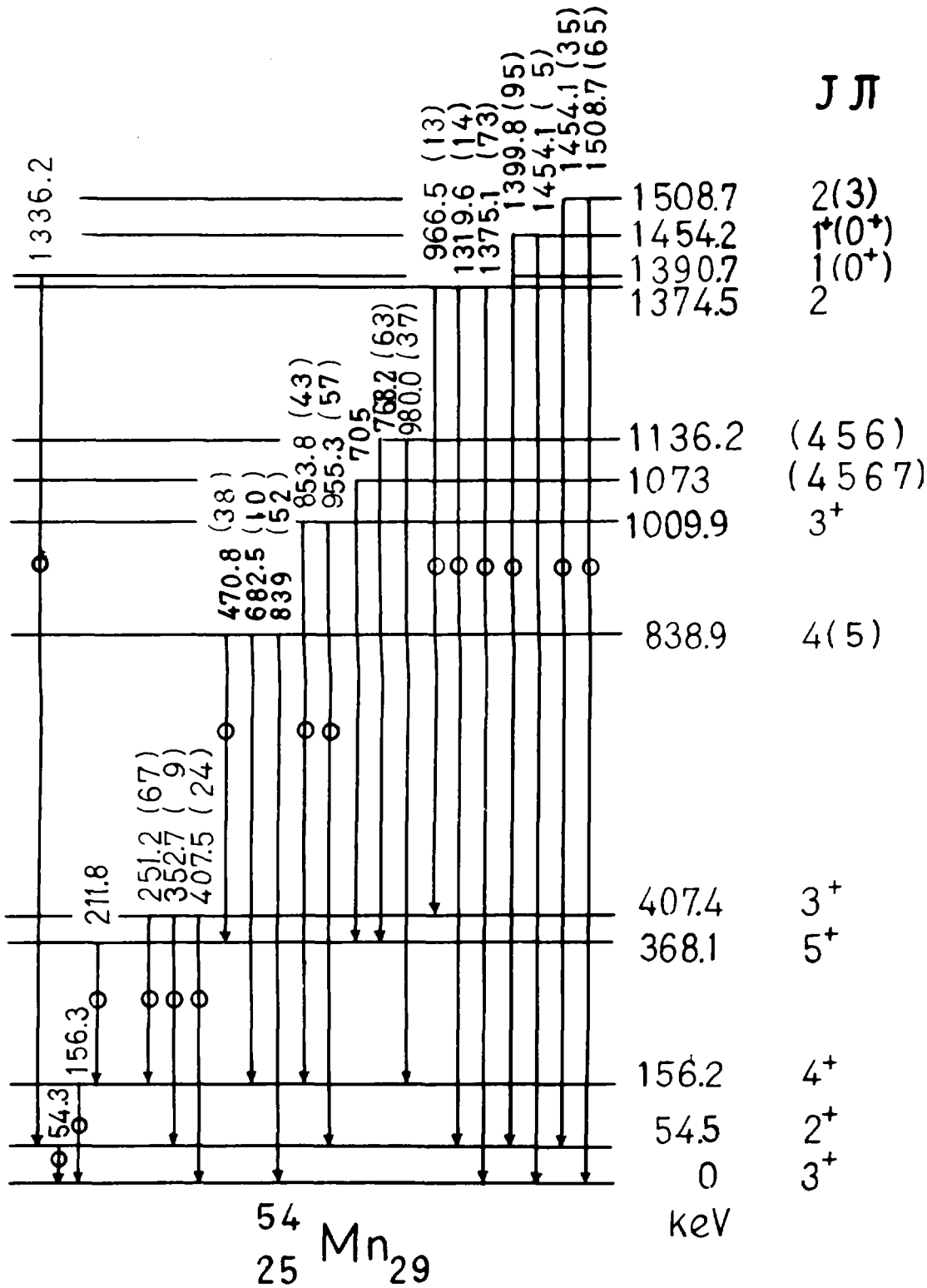

Fig. 7 Level scheme of ^{54}Mn obtained from the present work. Spin assignments were made using the results of the angular distributions and the excitation functions of γ-rays. Parities were determined from the other direct reactions. Gamma-ray branching ratios in parentheses beside γ-ray energies are given in %. Open circules show the γ-rays for which the angular distributions were measured.

Table 1 Summary of γ-ray angular distributions in the $^{54}Cr(p,n\gamma)$ reaction. The energy regions of incident protons are given in the second column of E_p. Spins and parities of the initial and final states for a transition are denoted by J_i and J_f respectively. Most probable spin sequences are given in the cases where unique spin-assignments were not obtained. Choices of transmission coefficients are given in the column of T^j_l. The optical-model parameter sets of V = 52 MeV, W = 11.5 MeV and V = 57 MeV, W = 13.5 MeV for protons are denoted by "52" and "57", respectively. For neutrons, the transmission coefficients from the optical-model parameters of Moldauer[4] are denoted by "M". The transmission coefficients tabulated by Bjorklund and Fernbach[5] and Perey and Buck[6] are denoted by "B+F" and "P+B", respectively. In the column of mixing ratio, E2-M1 mixing ratios are given for the respective sets of the transmission coefficients. In some cases, possible lower and upper limits of the mixing ratios are given in the parentheses instead of ordinary error representations. Most probable E2-M1 mixing ratios obtained from the weighted averages are given in last column.

E_γ keV	E_p MeV	A_2	A_4	$J_i^{\pi_i}$	$J_f^{\pi_f}$	T^j_l p	T^j_l n	mixing ratio δ		most probable δ
54	2.35-2.39	-0.1446 ±0.0087	+0.0080 ±0.0138	2^+	3^+	52	M	+0.184	±0.021	+0.10 $^{+0.11}_{-0.04}$
							B+F	+0.173	±0.020	
						57	M	+0.153	±0.018	
							B+F	+0.122	±0.014	
	2.45-2.49	-0.0758 ±0.0047	+0.0039 ±0.0076	2^+	3^+	52	M	+0.083	±0.012	
							B+F	+0.097	±0.013	
						57	M	+0.071	±0.010	
							B+F	+0.083	±0.012	
	2.55-2.59	-0.0697	+0.0022	2^+	3^+	52	M	+0.091	±0.014	
							B+F	+0.098	±0.015	
156	2.45-2.49	-0.3210 ±0.0438	-0.0716 ±0.0694	4^+	3^+	52	M	-0.022	±0.026	-0.030 $^{+0.05}_{-0.03}$
							B+F	-0.009	±0.025	
						57	M	-0.025	±0.028	
							B+F	-0.009	±0.025	
	2.55-2.59	-0.2994 ±0.0232	+0.0123 ±0.0368	4^+	3^+	52	M	-0.030	±0.017	
							B+F	-0.032	±0.017	
							P+B	-0.027	±0.016	
						57	M	-0.037	±0.017	
							B+F	-0.043	±0.017	
							P+B	-0.036	±0.016	
212	2.65-2.71	-0.3596 ±0.1344	-0.1775 ±0.2145	5^+	4^+	52	M	-0.033	±0.077	+0.038 $^{+0.03}_{-0.02}$
							B+F	-0.021	±0.071	
						57	M	-0.037	±0.078	
	2.80-2.82	-0.2002 ±0.0427	-0.0027 ±0.0676	5^+	4^+	52	M	+0.042	±0.025	
							B+F	+0.042	±0.025	
						57	M	+0.042	±0.025	
							B+F	+0.042	±0.025	
	2.94-2.98	-0.2001 ±0.0254	-0.0047 ±0.0400	5^+	4^+	52	M	+0.037	±0.016	
							B+F	+0.038	±0.015	
							P+B	+0.040	±0.014	
						57	M	+0.036	±0.016	
							B+F	+0.037	±0.016	
							P+B	+0.038	±0.016	
251	2.65-2.71	-0.1681 ±0.0111	-0.0044 ±0.0176	3^+	4^+	52	M	+0.037	±0.009	+0.023 $^{+0.03}_{-0.01}$
							B+F	+0.029	±0.008	
						57	M	+0.035	±0.009	
							B+F	+0.024	±0.008	
	2.80-2.82	-0.1174 ±0.0055	-0.0078 ±0.0088	3^+	4^+	52	M	+0.015	±0.006	
							B+F	+0.019	±0.006	
						57	M	+0.017	±0.006	
							B+F	+0.023	±0.007	
	2.94-2.98	-0.1019 ±0.0032	+0.0004 ±0.0051	3^+	4^+	52	M	+0.019	±0.004	
							B+F	+0.022	±0.004	
							P+B	+0.018	±0.004	
						57	M	+0.025	±0.004	
							B+F	+0.033	±0.004	
							P+B	+0.026	±0.005	

(continued)

E_γ keV	E_p MeV	A_2	A_4	$J_i^{\pi_i}$	$J_f^{\pi_f}$	T^j_1 p	n	mixing ratio δ		most probable δ
353	2.65-2.71	+0.0101 ±0.0472	+0.0056 ±0.0748	3^+	2^+	52	M	+0.19	±0.04	
							B+F	+0.19	±0.04	
						57	M	+0.19	±0.04	
	2.80-2.82	+0.0050 ±0.0298	-0.0180 ±0.0472	3^+	2^+	52	M	+0.18	±0.03	
							B+F	+0.18	±0.03	
						57	M	+0.19	±0.03	
							B+F	+0.19	±0.03	+0.18 +0.04 -0.03
	2.94-2.98	-0.0008 ±0.0165	+0.0257 ±0.0259	3^+	2^+	52	M	+0.18	±0.02	
							B+F	+0.18	±0.02	
							P+B	+0.18	±0.02	
						57	M	+0.18	±0.02	
							B+F	+0.18	±0.02	
							P+B	+0.18	±0.02	
407	2.65-2.71	+0.4077 ±0.0186	+0.0348 ±0.0294	3^+	3^+	52	M	+0.060	±0.030	
							B+F	+0.023	±0.025	
						57	M	+0.049	±0.028	
							B+F	+0.002	±0.024	
	2.80-2.82	+0.3402 ±0.0128	-0.0002 ±0.0203	3^+	3^+	52	M	+0.058	±0.024	
							B+F	+0.081	±0.027	
						57	M	+0.070	±0.025	
							B+F	+0.105	±0.029	+0.060 +0.09 -0.08
	2.94-2.98	+0.2807 ±0.0099	+0.0007 ±0.0155	3^+	3^+	52	M	+0.047	±0.022	
							B+F	+0.065	±0.023	
							P+B	+0.042	±0.021	
						57	M	+0.079	±0.024	
							B+F	+0.12	±0.03	
							P+B	+0.087	±0.026	
471	3.35-3.39	-0.0667 ±0.0677	-0.0413 ±0.1072	4^+	5^+	52	M	-0.045	±0.065	-0.045 ±0.07
						57	M	-0.045	±0.068	
						52	M	-7.7	(-17,-5.2)	-8 +3 -9
						57	M	-9.0	(-17,-5.2)	
				5^+	5^+	52	M	-0.73	±0.15	-0.7 ±0.2
						57	M	-0.72	±0.18	
854	3.35-3.39	-0.1854 ±0.0142	+0.0033 ±0.0224	3^+	4^+	52	M	+0.049	±0.012	
							B+F	+0.040	±0.011	+0.042 ±0.02
						57	M	+0.047	±0.013	
							B+F	+0.036	±0.011	
955	3.35-3.39	-0.2361 ±0.0100	+0.0759 ±0.0158	3^+	2^+	52	M	+0.038	±0.006	
							B+F	+0.046	±0.006	
						57	M	+0.038	±0.006	
							B+F	+0.049	±0.006	+0.044 +0.04 -0.02
	3.80-3.84	-0.1267 ±0.0150	-0.0048 ±0.0238	3^+	2^+	52	M	+0.064	±0.014	
						57	M	+0.056	±0.014	
967	3.80-3.84	-0.2191 ±0.0713	+0.0457 ±0.1130	2^+	3^+	52	M	+0.18	±0.09	
							B+F	+0.22	±0.11	+0.18 ±0.1
						57	M	+0.16	±0.09	
							B+F	+0.18	±0.10	
						52	M	+100	(+10,-14)	
							B+F	+ 25	(+ 7,-18)	$\lvert\delta\rvert>10$
						57	M	-100	(+13,-11)	
							B+F	+100	(+10,-14)	

(continued)

E_γ keV	E_p MeV	A_2	A_4	$J_i^{\pi_i}$	$J_f^{\pi_f}$	T^j_l p	n	mixing ratio δ		most probable δ
1320	3.80-3.84	+0.4817 ±0.0769	+0.1270 ±0.1219	2^+	2^+	52	M	+0.96	(+1.36,+0.70)	
								+0.40	(+0.70,+0.22)	+0.4 +0.3 -0.2
							B+F		(+1.15,+0.32)	
						57	M	+1.1	(+1.5, +0.70)	
								+0.32	(+0.70,+0.18)	+1.0 +0.5 -0.3
							B+F	+0.92	(+1.24,+0.70)	
								+0.45	(+0.70,+0.22)	
1336	3.80-3.84	+0.0183 ±0.0036	-0.0012 ±0.0057	1^+	2^+	52	M		(-1.1,-0.45)	
							B+F		(-1.1,-0.45)	(-0.4,-1.3)
						57	M		(-1.3,-0.40)	
							B+F		(-1.3,-0.40)	
1375	3.80-3.84	-0.0747 ±0.0148	-0.0060 ±0.0234	2^+	3^+	52	M	<0.001	±0.019	
							B+F	+0.010	±0.020	+0.002 ±0.02
						57	M	-0.005	±0.018	
							B+F	+0.002	±0.019	
						52	M	-5.8	(-6.5,-5.3)	
							B+F	-6.5	(-7.4,-5.8)	-6.0 +1.4 -0.8
						57	M	-5.8	(-6.6,-5.2)	
							B+F	-6.0	(-6.9,-5.4)	
1400	3.80-3.84	-0.0017 ±0.0037	+0.0089 ±0.0058	1^+	2^+	52	M	-0.045	(-0.11,+0.02)	
							B+F	-0.045	(-0.11,+0.02)	-0.05 +0.07 -0.06
						57	M	-0.050	(-0.11,+0.015)	
							B+F	-0.050	(-0.11,+0.015)	
						52	M	-2.8	(-3.6,-2.3)	
							B+F	-2.8	(-3.6,-2.3)	-2.8 +0.5 -0.8
						57	M	-2.8	(-3.6,-2.4)	
							B+F	-2.8	(-3.6,-2.4)	
1454	3.80-3.84	+0.3361 ±0.1156	-0.0671 ±0.1832	2^+	2^+	52	M	+0.015	(+0.15,-0.11)	
							B+F	+0.025	(+0.17,-0.10)	+0.01 +0.16 -0.13
						57	M	+0.001	(+0.13,-0.12)	
							B+F	+0.001	(+0.13,-0.12)	
						52	M	+2.2	(+3.1,+1.6)	
							B+F	+2.1	(+3.0,+1.5)	+2.2 +1.0 -0.7
						57	M	+2.3	(+3.2,+1.6)	
							B+F	+2.3	(+3.2,+1.6)	
1509	3.80-3.84	-0.0849 ±0.0268	+0.0094 ±0.0424	2^+	3^+	52	M	-0.007	±0.026	
							B+F	-0.005	±0.028	-0.008 ±0.03
						57	M	-0.011	±0.026	
							B+F	-0.010	±0.026	
						52	M	-5.6	(-6.6,-4.8)	
							B+F	-5.6	(-6.6,-4.8)	-5.6 +0.8 -1.0
						57	M	-5.5	(-6.5,-4.8)	
							B+F	-5.5	(-6.5,-4.8)	

VI. University of Tokyo
Institute of Physics, College of General Education

VI-1. Microscopic Description of Scattering of Low Energy Neutrons by ^{12}C : I*

A. Mori** and T. Terasawa

Abstract: The total cross section for the elastic scattering of neutrons by ^{12}C up to E_n = 4.4 MeV is calculated by the coupled channel method. A coupling form factor is constructed from a microscopic wave functions of ^{12}C and a realistic two-body interaction between the incident neutron and a nucleon of the target. The renormalization of the interaction strength is found to be necessary, which is discussed in connection with antisymmetrization effects.

---

* Prog. Theor. Phys. 48 (1972) No.3 (in press).

** Present Address: Dept. of Phys., Tokyo Institute of Technology.